



Review

Luminescent and chromogenic molecular probes based on polyamines and related compounds

Carlos Lodeiro^{*,1}, Fernando Pina¹

REQUIMTE, Departamento de Química, Faculdade de Ciências e Tecnologia, Universidade Nova de Lisboa, 2829-516 Monte de Caparica, Portugal

Contents

1. Introduction.....	1353
2. Polyamine-based receptors.....	1355
3. Sensing units.....	1356
3.1. Aromatic hydrocarbon atoms.....	1356
3.1.1. "ON-OFF" switch based on excimer emission driven by light.....	1356
3.1.2. Exciplex involving complexation with metals.....	1357
3.1.3. Intramolecular energy transfer: switching from ET to eT by the action of metals or protons.....	1360
4. Receptor unit.....	1361
4.1. Phenanthroline, bipyridine and terpyridine units.....	1362
5. Applications.....	1366
5.1. Exploring the photocatalytic properties.....	1366
5.2. Sensing anions.....	1367
5.3. Antenna effect.....	1367
5.4. Sensing ATP by metal complexes.....	1369
6. Oxa-aza-based receptors: Schiff-base and amine ligands with N _x O _y donor sets.....	1370
7. Emissive polythia-aza-based receptors.....	1374
8. Chromogenic complexes containing sulfur donor receptors for recognition effects.....	1379
9. Conclusions and outlook.....	1381
Acknowledgements.....	1381
References.....	1381

ARTICLE INFO

Article history:

Received 16 May 2008

Received in revised form

11 September 2008

Accepted 11 September 2008

Available online 23 September 2008

Keywords:

Polyaza receptors
Oxa-aza receptors
Thia-aza receptors
Chemosensors
Fluorescence
Colorimetric

ABSTRACT

This review describes some developments on the coordination chemistry of chemosensors based on polyamines and related compounds, with particular emphasis on their photochemical properties. The reported systems are essentially based on the work developed by the authors since 2000. Some interesting properties beyond sensing molecules and/or atoms by fluorescence or colorimetry can arise from these systems. In particular pH and light can be used as external stimuli to carry out functions, like molecular movements, jumping of metal ions inside-outside polyaza cavities, photocatalytic effects, energy and electron transfer.

© 2008 Elsevier B.V. All rights reserved.

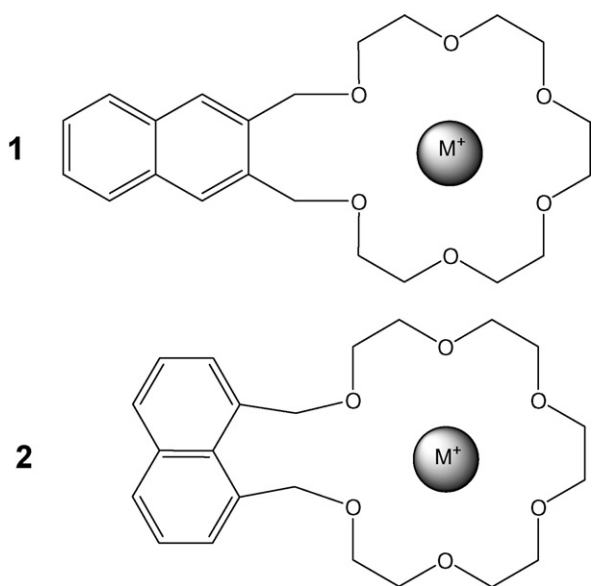
1. Introduction

The detection and control of analytes comprising cations and anions is an essential task in many of the human activities, from agriculture, food, and environment sciences, to medicine and health sciences. It is easy to predict an increasing demand of devices capa-

* Corresponding author. Tel.: +351 212948300; fax: +351 212948550.

E-mail address: lodeiro@dq.fct.unl.pt (C. Lodeiro).

¹ Both authors contributed equally to this work.



Scheme 1.

cence and phosphorescence of compounds **1** and **2** by alkali metal cations (Scheme 1). While in compound **1** (ethanol glass at 77 K) the fluorescence quantum yield is quenched, and the phosphorescence quantum yield is enhanced by these metals, in compound **2** it is exactly the contrary, the fluorescence is enhanced and the phosphorescence quenched [1].

Sousa's work presented for the first time in compound **2**, the enhancement of the fluorescence of an aromatic hydrocarbon system by the addition of "perturbers" which are held in a pre-determined orientation without the use of a covalent bond.

The concept of "switching on" was introduced by A. P. de Silva, in 1986, to characterize the large perturbation caused by the addition of Na^+ and K^+ to methanol solutions of compound **3**, Scheme 2. In this compound the anthracene fluorescence is quenched by electron transfer from the lone pair of the nitrogen, and is recovered on incorporation (recognition) of the alkali metal-ion into the macrocycle [2].

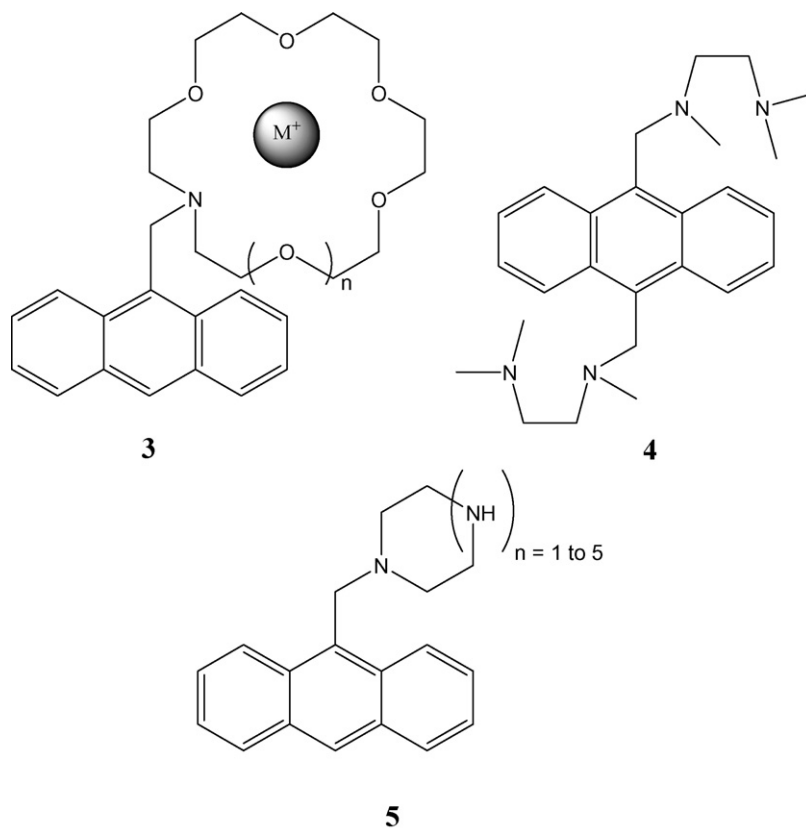
Recovery of the anthracene fluorescence emission was also described by Czarnik in Ref. [3]. This author reported the chelation-enhancement of fluorescence (CHEF) that occurs upon Zn^{2+} coordination to compound **4**, see Scheme 2. The lack of fluorescence emission in this compound is attributed to a quenching process by electron transfer, taking place from the lone pairs of the amine to the excited fluorophore. Protonation of the amines or coordination of some metals (d^{10}) such as Zn^{2+} or Cd^{2+} prevents the electron transfer process, allowing the fluorophore to exhibit its intrinsic fluorescence.

The concept of chemosensor was clearly defined by Czarnik [4], as a molecule containing a binding site (receptor), a fluorophore (sensing), and a mechanism for communication between the two (through the spacer) see Scheme 3.

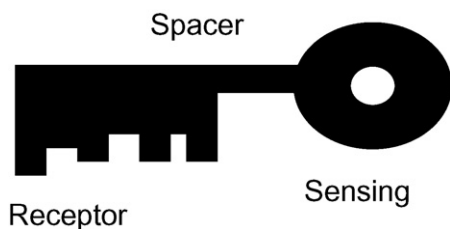
Many reviews concerning acyclic or macrocyclic ligands for metal ion complexation and detection have been published

ble of sensing and controlling different analytes taking profit from the great computing capacity nowadays accessible. Thus, the search for compounds whose properties are modified in the presence of a target compound is a matter of great interest. One expeditious way to sense analytes is the use of chemosensors, in particular those exhibiting fluorescence, due to low detection limit and easy accessibility of this technique.

The concept of chemosensor was reported for first time by L. R. Sousa in 1977. He described the perturbation of the fluores-



Scheme 2.



Scheme 3.

recently, some of them, with an exhaustive presentation of compounds used for the synthesis of polynuclear metal complexes [5,6]. Application of metal complexes as fluorescence [7] and colorimetric [8], chemosensors has been also exhaustively reviewed due to the increased interest in these multifunctional materials.

In this review we summarized the contributions from our group to the chemosensor field, emphasizing chemosensors based on polyamine receptors capable of operating in water, the ubiquitous solvent, in particular concerning the biological systems. The interactions with metal ions, anions and with protons are discussed, together with some interesting functions linked to response of the system to external stimuli such as light and pH.

2. Polyamine-based receptors

The first water-soluble chemosensor possessing a polyamine macrocycle receptor linked to an aromatic hydrocarbon was

reported in 1990 by Czarnik and co-workers compound **5**, Scheme 2 [9]. In this example, protons, as well as Zn^{2+} and Cd^{2+} , switch ON the fluorescence of the sensor.

The presence of the polyamine receptor unit usually renders the sensor water-soluble, in great part due to the protonation equilibria undergone by the polyamine in water. Speciation of the sensor leads to the presence of an ensemble of forms that can be selected for optimum detection performance for a given analyte. For instance, the protonation of the polyamine at acidic pH values renders an anionic sensor while at basic pH the unprotonated forms are ideal to complex metal ions.

The polyamine receptors can be built using cyclic or linear chains. In some cases two and more linear chains have been used. Examples of all these receptors will be given through this review.

Anthracene and naphthalene were the first fluorescent sensing units to be explored [9] but other alternatives were considered later, as for example dansyl [10], 8-hydroxyquinoline [11] and ruthenium tris-bipyridine derivatives [12]. In all cases the fluorescence emission of the sensing unit should be increased or decreased upon binding of the analyte to the receptor.

Concerning the mechanisms through which the chemosensor operates, photo-induced electron transfer (PET) involving the excited sensing unit and the polyamine receptor is the most common. In the case of anthracene and naphthalene the PET occurs from the lone pair of the nitrogen atoms to the excited fluorophore. In some receptor units, aromatic nitrogen heterocycles like pyridine, phenanthroline or bipyridine have been integrated into the receptor unit to modulate the binding properties. In these cases,

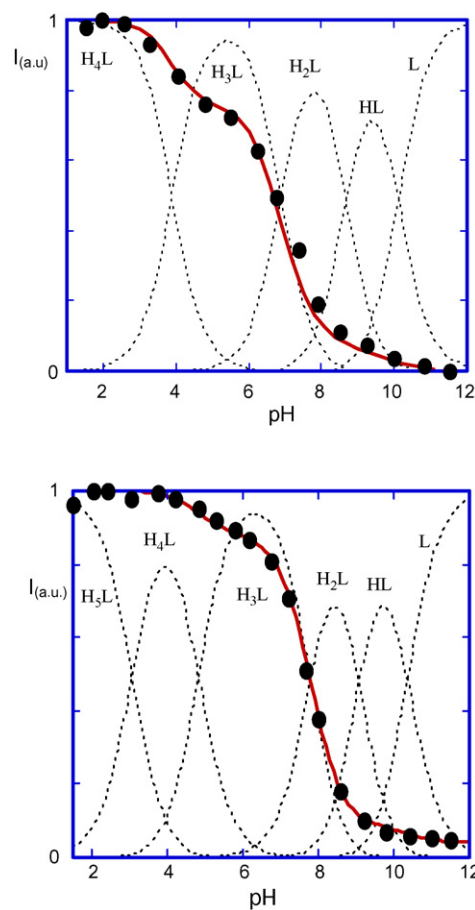
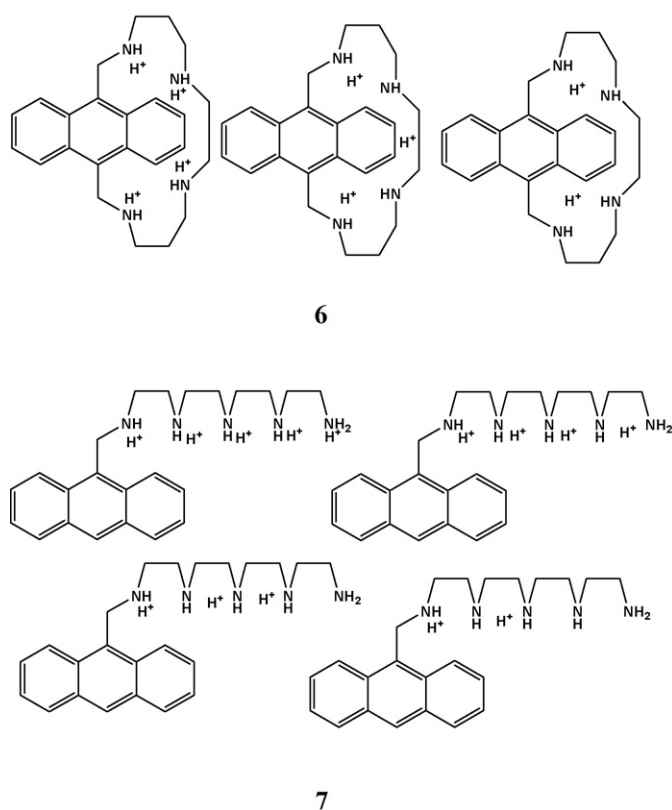


Fig. 1. Fluorescence emission titration curves of two representative polyamine-based sensors, compounds **6** and **7**, superimposed with the mole fraction distribution of the species obtained by potentiometry [21].

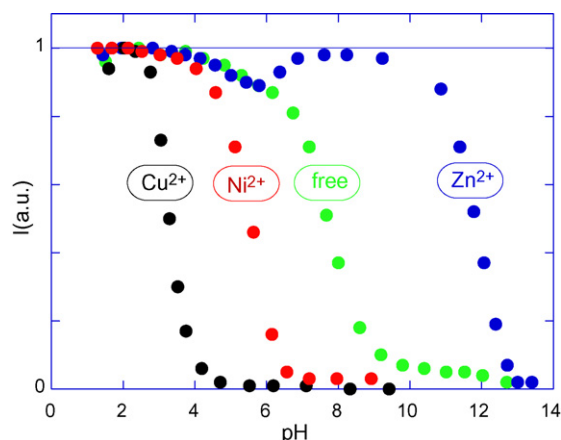


Fig. 2. Comparison of the fluorescence emission of compound **7** at 420 nm for the various metal ions [21].

protonation of the aromatic nitrogen at acidic pH values also gives rise to PET from the excited fluorophore to the protonated heterocycle, resulting in fluorescence quenching. Systems containing both aliphatic amines and nitrogen heterocycles are only effective in a pH window whose width is dependent on the structure of the molecule [13–17]. More recently oxygen and sulfur atoms have been integrated into the polyaza chains in order to render the receptor unit more versatile [18].

In collaboration with García-España we introduced in 1995, for the first time, the systematic superposition of the potentiometric and fluorescence emission titration curves, to study the interaction of polyazacyclophane macrocyclic receptors, with the anion, hexacyanocobaltate(III) [19]. This approach was later on complemented by the use of NMR titrations [20]. These three combined techniques, fluorescence emission, potentiometry, and NMR, used as a function of pH, proved to be a powerful tool to investigate the behaviour in water of fluorescent polyamine chemosensors. In particular, this approach permits in the majority of the cases to assign the sequence in which the nitrogen atoms of the polyamine are protonated, and thus clearly identify the contribution of each species to the fluorescence emission, at each pH value.

An example of this strategy is reported in Fig. 1. The relative contribution of each species can be measured. The maximum of the fluorescence emission is observed for the more protonated forms, because protonation prevents the quenching process by electron transfer and in contrast at high pH values the emission is not observed, due to the PET quenching process.

Compounds like those reported in Fig. 1 (compounds **6** and **7**) can be used also to sense transition metals [21]. As an example in the case of the chemosensor bearing a linear chain (compound **7**) the stability constants for the respective complexes with Copper, Zinc and Nickel follows a tendency, $\text{Cu}^{2+} > \text{Ni}^{2+} > \text{Zn}^{2+}$, as expected from the general Irving-Williams order of stability for octahedral complexes. In Fig. 2 the fluorescence emission titration curve of the complexes formed between compound **7** and equimolar quantities of the metal cations is shown.

The different behaviour of the fluorescence emission in the presence of these metals can be used to define logic gates [21]. As an example, if the fluorescence emission is the output signal of the system and 0 is considered the absence of the metal and 1 its presence the following logic table can be defined for the pair zinc and copper [21] (Table 1).

Other combinations can be defined leading to different logic tables as reported in Ref. [21].

Table 1

Logic gates defined with the fluorescence emission of compound **6** at 420 nm for Zn^{2+} and Cu^{2+} [21].

Zn^{2+}	Cu^{2+}	pH 5	pH 10
0	0	1	0
0	1	0	0
1	0	1	1
1	1	0	0
		NOT Cu^{2+}	NOT ($\text{Zn}^{2+} \Rightarrow \text{Cu}^{2+}$)

3. Sensing units

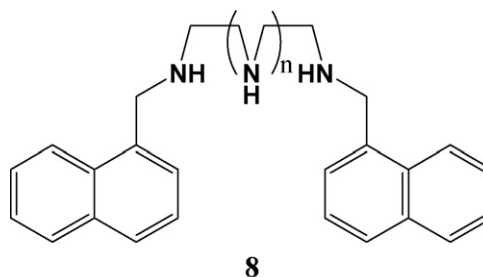
3.1. Aromatic hydrocarbon atoms

The sensing unit plays a central role in the performance of the chemosensor. Aromatic hydrocarbon atoms have been extensively used, due to their good fluorescence emission quantum yields and because they can easily communicate with the polyamine receptor through PET. In the cases where the sensing unit possesses two or more chromophores, as an example see compound **8** (Scheme 4), formation or disappearance of intramolecular excimers can be used together with the monomer emission to sensing target compounds [22].

3.1.1. “ON-OFF” switch based on excimer emission driven by light

The first water-soluble chemosensor based on excimer emission was claimed by Van Arman and co-workers [23]. These authors reported the anthracene excimer emission of a bis-chromophoric compound upon coordination with Zn^{2+} .

More recently a systematic study of these bis-chromophoric species containing chains with different lengths was carried out using the three combined techniques mentioned above [24,25]. The fluorescence emission titration curve was superimposed to the mole fraction distribution of the several species in solution, obtained by potentiometry, see for example Fig. 3 for $n=1$. The protonation sequence in this case is easy to predict and can be confirmed by the chemical shifts of the protons (^1H) and carbon atoms (^{13}C): the first proton goes to one of the terminal nitrogen atoms, the second one to the other terminal nitrogen, in order to maximize the electrostatic repulsion and finally the third to the central nitrogen. The absorption spectra are practically independent on the protonation sequence, but in contrast the fluorescence emission is dramatically affected, see Fig. 3A. The excimer emission is clearly identified by the observation of its red shifted and unstructured emission band. Full protonation of the polyamine receptor prevents PET and confers rigidity to the chain: by consequence H_3L^{3+} exhibits the highest fluorescence emission intensity and no excimer emission. Removal of the first proton from the central nitrogen is enough to confer a larger flexibility to the polyamine chain, allowing excimer formation, as well a decrease of the monomer emission by PET from the central amine to the excited naphthalene. Complete



Scheme 4.

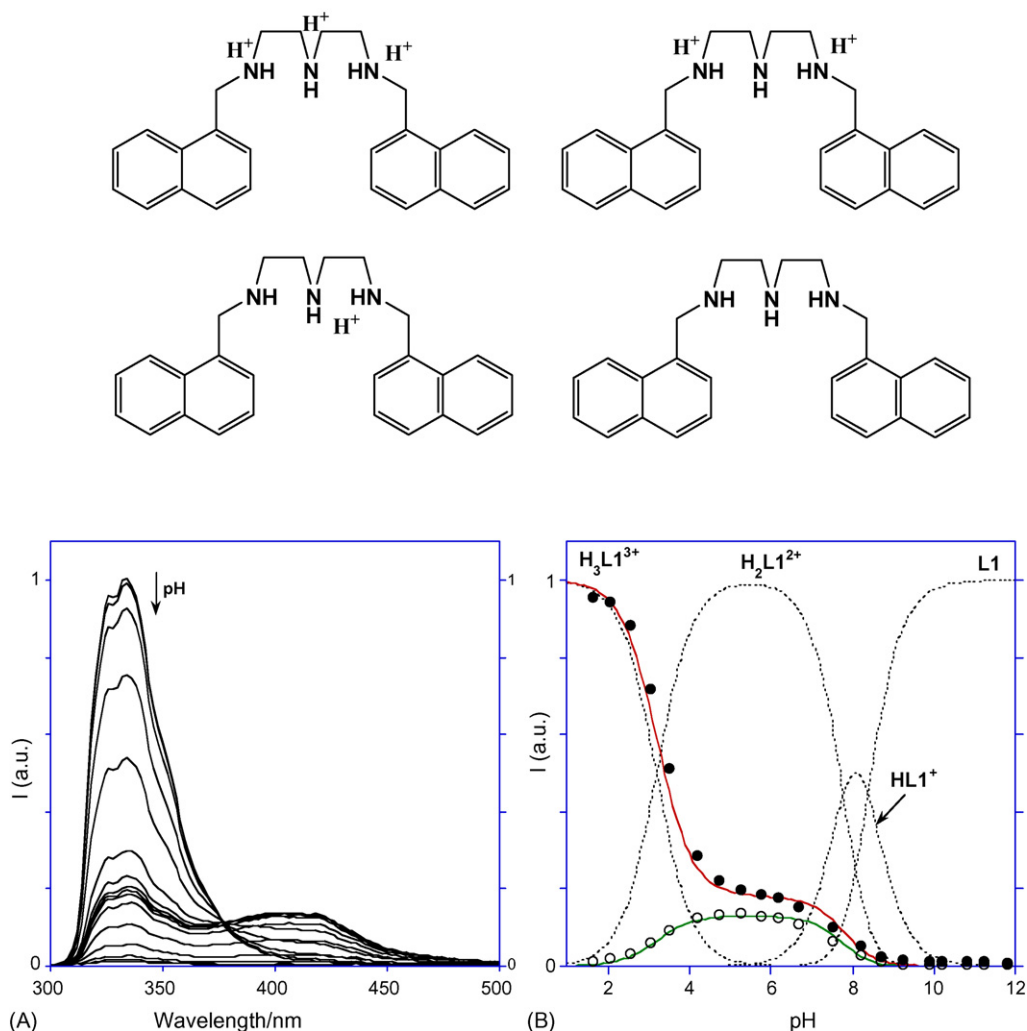


Fig. 3. (A) pH dependence of the fluorescence emission of compound **8** $\lambda_{\text{exc}} = 280$ nm. (B) Mole fraction distribution of the protonation states of compound **7**: (●) fluorescence emission at $\lambda_{\text{exc}} = 280$ nm and $\lambda_{\text{em}} = 334$ nm; (○) Fluorescence emission at $\lambda_{\text{exc}} = 280$ nm and $\lambda_{\text{em}} = 418$ nm [24,25].

quenching can only occur when a second proton is taken off from the polyamine chain.

Further evidence for this interpretation can be found from the fluorescence emission of a mono-chromophoric species, Fig. 4. In this case there is neither excimer formation, nor any significant indication of the exciplex emission, as expected, because the solvent is water. In addition, if a piperazine unit is introduced in the chain to confer rigidity, the excimer is not formed in spite of the existence of two terminal naphthalene units, Fig. 4.

In Scheme 5 the ON-OFF properties of compound **8** regarding the output signal of its excimer emission, are summarized. At pH 2.0 the system is locked and there is no chance to form the excimer due to the rigidity of the chain, OFF state. When the system is unlocked to pH 6.0, the excimer emission can be observed and the system is ON.

Formation of excimer was also described for compounds **9** and **10** (Scheme 6) [26]. The different central spacer unit with different connections to the central benzene groups with the polyamine chain, leads to small but significant differences in the photophysical behaviour of the two compounds, namely in the rate of excimer formation at acidic pH values. Excimer formation at acidic pH values when the protonation of the polyamine bridges is extensive (all six secondary amines) is noted. Identically excimer emission was detected for compound **11**. In this case time-resolved fluorescence

data, obtained by single photon counting showed that a significant percentage of excimer is performed as ground state dimers [27].

Complexation of compound **11** with Cu^{2+} and Zn^{2+} showed the formation of mono- and dinuclear complexes in which the nitrogen atoms in the pendant arms do not provide a strong contribution to the overall stability. In both cases excimer emission is not observed. Copper complexation gives rise to a Chelation Enhancement of Quenching (CHEQ) effect while zinc complexation originates a slight CHEF effect. The lack of significant CHEF effect expected upon coordination of this last metal was attributed to a compensating effect due to the participation of the pyridine units in the Zn^{2+} complexation that is expected to give a CHEQ effect [27].

3.1.2. Exciplex involving complexation with metals

Sensing metal ions upon complexation can be achieved by the fluorescence emission not only from excimers but also from exciplexes. The coordination environment re-organizes the structure of the ground and excited states of the chemosensor, in some cases inducing in other cases preventing the formation of these excited state species.

An example of this behaviour was found with the Zn^{2+} complex of compound **12** [28,29]. Coordination/detachment of a pendent functionality in the Zn^{2+} complex with the macrocyclic ligand **12** gives rise to on/off switching of exciplex emission, defining an ele-

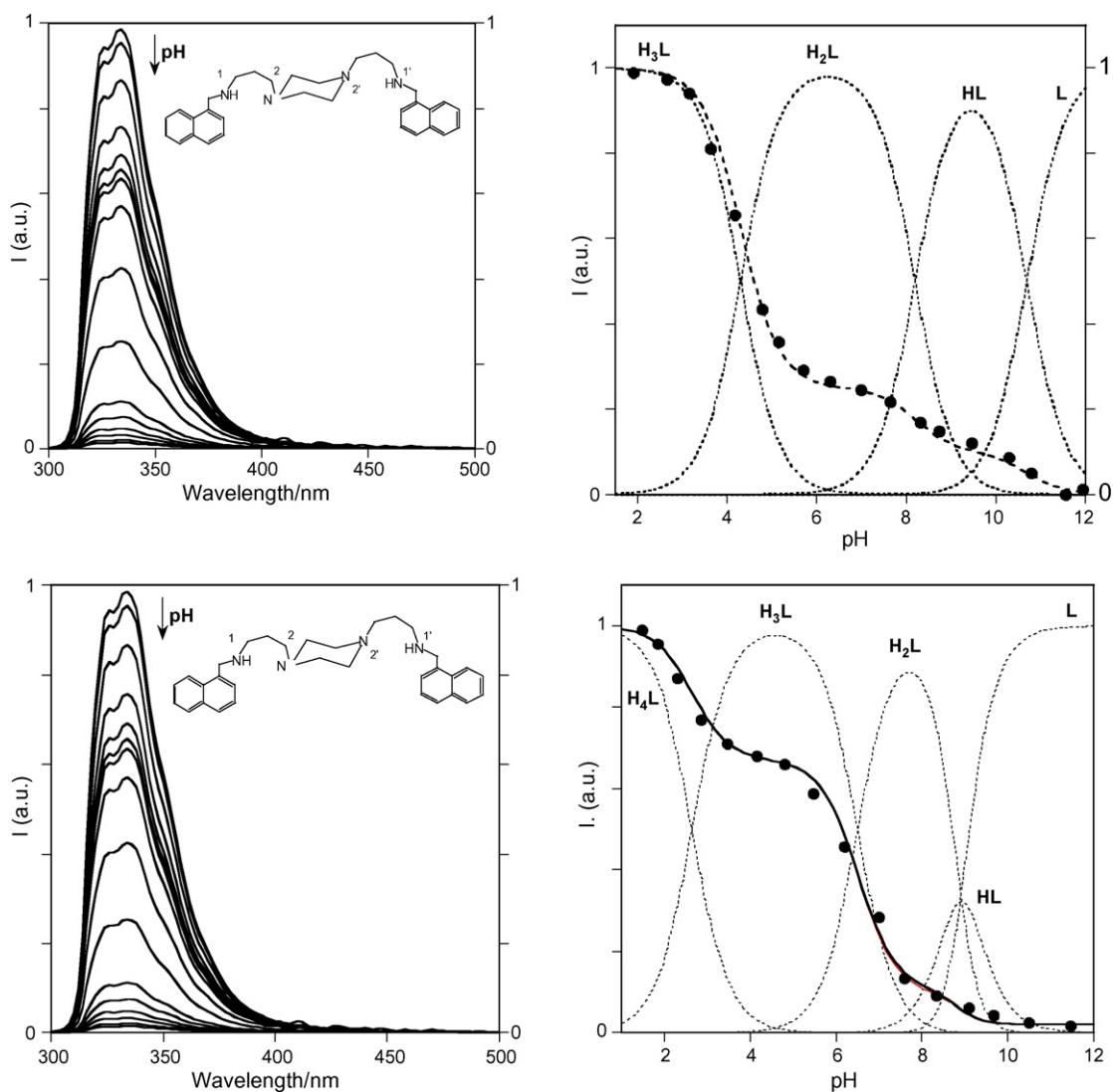
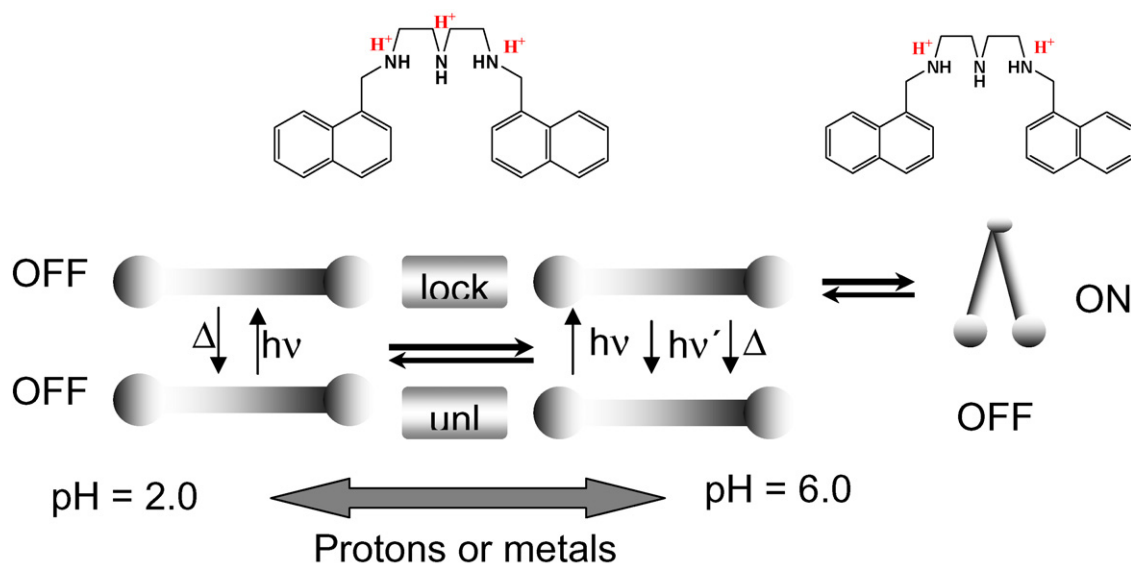


Fig. 4. pH dependence of the fluorescence emission at $\lambda_{\text{exc}} = 280$ nm. (A) Mole fraction distribution of the protonation states: (●) fluorescence emission at $\lambda_{\text{exc}} = 280$ nm and $\lambda_{\text{em}} = 334$ nm. (A) mono-chromophoric and (B) bis-chromophoric [24,25].



Scheme 5.

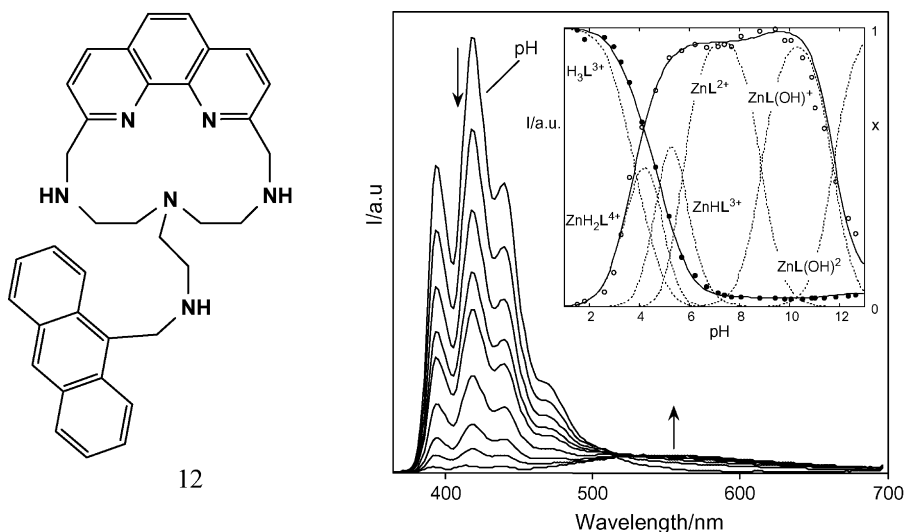


Fig. 5. Fluorescence emission spectra of the Zn^{2+} (**12**) (1:1) system in 0.15 M NaCl $\text{CH}_3\text{CN}:\text{H}_2\text{O}$ 1:1 (v:v) at different pH values: 1.69; 3.73; 4.4; 4.87; 5.1; 5.57; 6.05; 6.55, 10.37 ($\lambda_{\text{exc}} = 352$ nm). Inset: fluorimetric titration of the same system: (●) emission followed at 418 nm; (○) exciplex emission followed at 600 nm. Species distribution curves (inset) represent mole fractions [28,29].

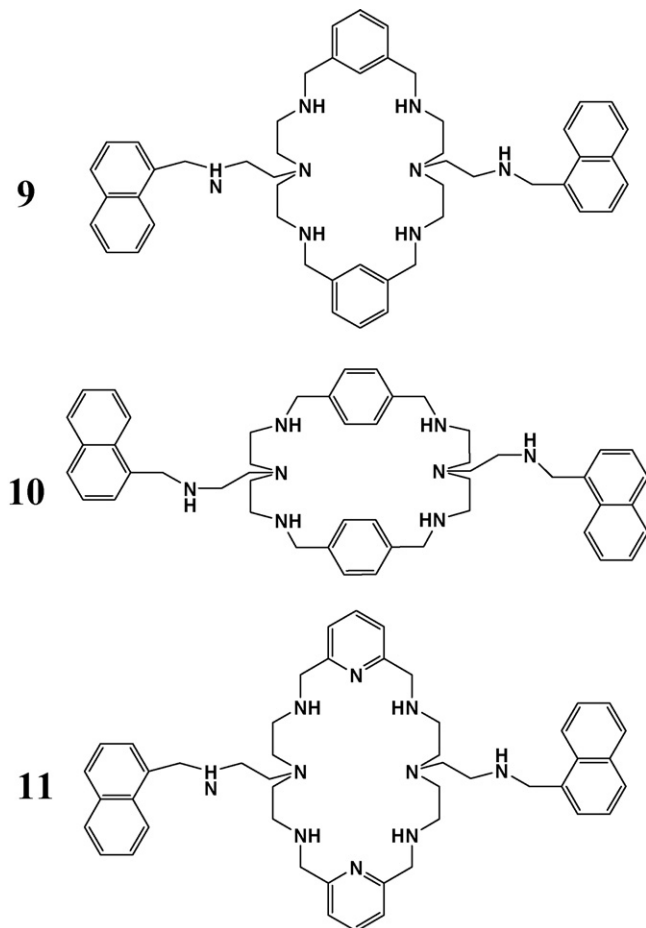
mentary molecular machine whose movements can be driven by both, pH and light (Fig. 5).

Steady-state and time-resolved fluorescence studies with the Zn^{2+} complex of **12** were reported in solution (ethanol) and in the solid state. In solution from the temperature dependence of

the photostationary ratio ($I_{\text{exc}}/I_{\text{M}}$), the activation energy for exciplex formation ($E_a = 12.3 \text{ kJ mol}^{-1}$) and the binding energy of the exciplex ($\Delta H = -7.9 \text{ kJ mol}^{-1}$) were determined (see Fig. 6).

In the solid state, the absorption spectrum of a thin film of **12** is red-shifted relative to the solution spectra whereas its emission spectrum reveals the unique featureless exciplex band but blue shifted relative to solution. In conjunction with X-ray data (see Fig. 7) the solid-state data were interpreted as being due to a new exciplex where differently from the results in water no π -stacking (full overlap of the p-electron cloud of the two chromophores-phenanthroline) is observed.

Further clear evidence for an exciplex emission was obtained in compound **13** (Scheme 7) [30]. In this case the exciplex emission is centred ca. 430 nm, compared with the excimer $\lambda_{\text{max}} = 418$ nm, reaches its maximum at pH 6, and was interpreted as an exciplex-like structure involving the naphthalene and one of the pyridine units. There is no possibility of intramolecular excimer formation and the intermolecular excimer can be excluded due to the low



Scheme 6.

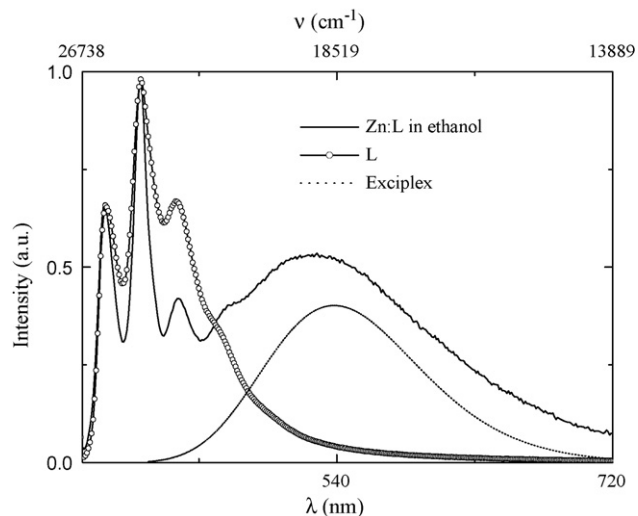


Fig. 6. Fluorescence emission spectra $\lambda_{\text{exc}} = 352$ nm of the $\text{Zn}(\text{12})$ complex in ethanol at 293 K. The exciplex band results from the subtraction of the emission spectra of **12** and that of the complex [29].

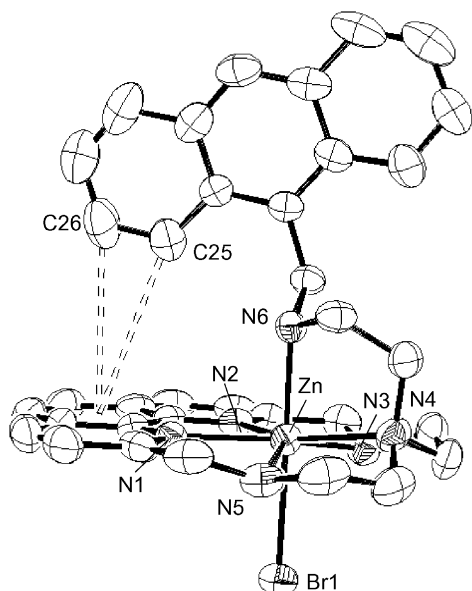
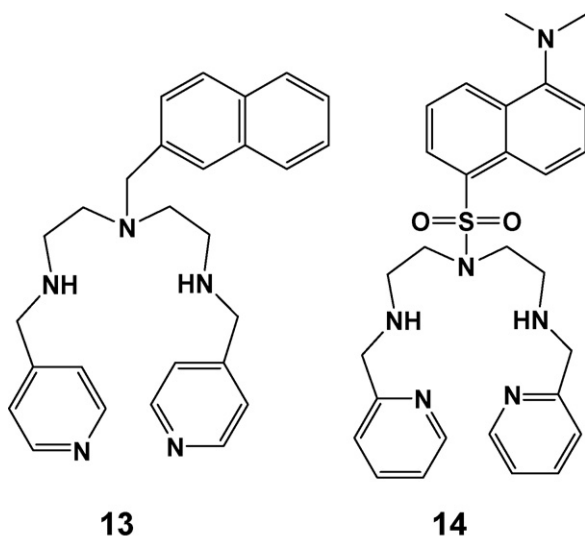


Fig. 7. ORTEP drawing of the $[Zn(12)Br]^+$ complex cation [29].

concentrations used and the lack of changes on the intensity of this band in the range 10^{-5} to 10^{-6} M.

Complexation with Zn^{2+} leads to a total disappearance of the exciplex emission. According to this data, Zn^{2+} can be detected by the fluorescence emission intensity of its complex with **13**, in a very narrow pH window centered *ca.* pH 8.0.

In contrast with the chemosensors bearing naphthalene (or anthracene) sensing units, those presenting the dansyl fluorophore are emissive only at basic pH value, because the protonated form of the dansyl unit is not emissive. In contrast with the usual behaviour for Zn^{2+} complexes in the case of ligand **14** (Scheme 7), strong coordination with the metal takes place accompanied by a relatively strong quenching of the fluorescence [31]. The quenching effect was related to the coordination of the metal to the pyridine groups, by analogy with identical quenching of naphthalene or anthracene by pyridines complexed with Zn^{2+} . When the **Zn14** complex is irradiated an intense and blue shifted emission band, is formed, Fig. 8.



Scheme 7.

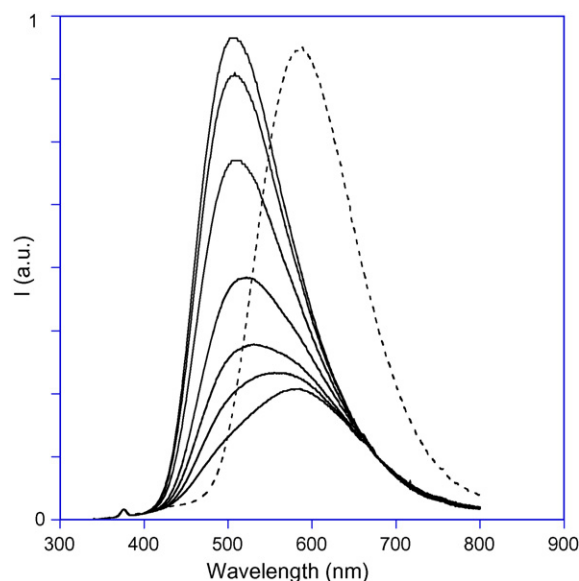


Fig. 8. Irradiation of the compound $Zn(14)^{2+}$ at 333 nm, pH 7.3: 0, 5, 10, 15, 20, 25, and 30 min, full lines; free ligand (traced line) 5.0×10^{-5} M, $[NaCl] = 0.15$ M [31].

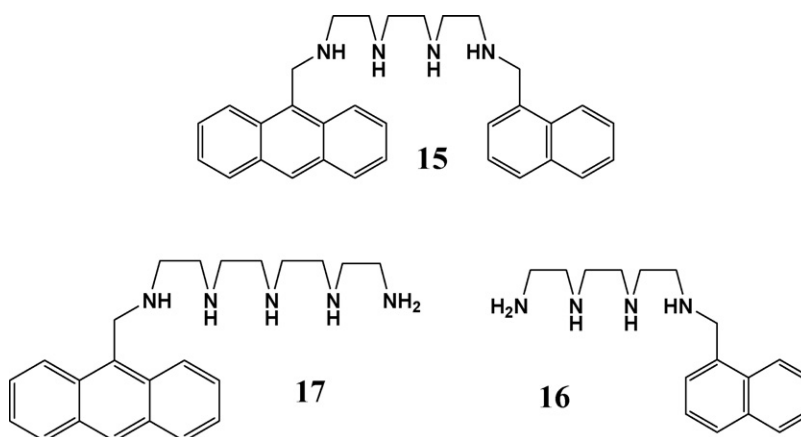
A similar spectroscopic feature was previously described by Kimura and co-workers on model compounds for Zn^{2+} enzymes as a result of formation of strong bonds between aromatic sulfonamides and Zn^{2+} [32]. In particular, a fluorophore possessing a cycle receptor unit and a dansyl signalling moiety was shown to exhibit such behaviour at pH 7.3. The dansylsulfonamide is deprotonated and the nitrogen binds strongly to the metal, leading to a blue shifted new fluorescence emission band whose intensity increases *ca.* five-fold. In compound **14**, the nitrogen of dansylsulfonamide is tertiary but there is still an electron pair available to coordinate the metal. Although this is not the usual situation in the ground state, there are some reports on tertiary sulfonamide binding to metal ions. Taking into account that the excited dansyl unit is reached from a charge transfer from the dimethylamino-substituted aromatic moiety to the sulfonamide, the excess of charge in this nitrogen in the excited state might be the driving force to remove water from the intimate coordination sphere of the metal and give rise to a bond. The bond Zn^{2+} -dansylsulfonamide, would lead to a similar fluorescence pattern as found by Kimura and co-workers [32].

3.1.3. Intramolecular energy transfer: switching from ET to eT by the action of metals or protons

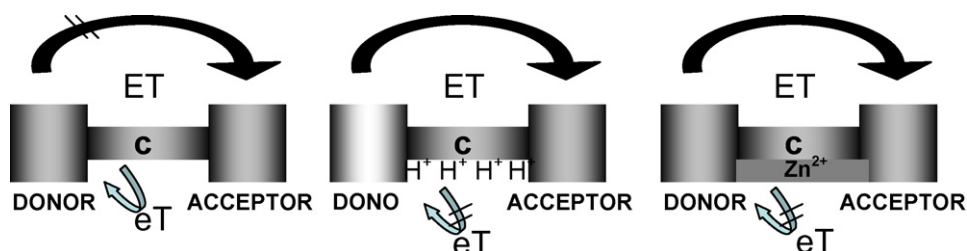
Covalently linked donor-acceptor (CLDA) systems is a subject of great interest because of the theoretical and practical applications of electron (eT) and energy transfer (ET) that can take place in these molecules. Compound **15** has been synthesized using a polyamine chain to link a donor and an acceptor, as shown in Scheme 8 for compound **15** [33].

In order to maximize the energy transfer process, the polyamine chain must be fully protonated, otherwise electron transfer quenches the emission as was mentioned above for other similar polyamine compounds. System **15** allows selective excitation of each fluorophore: anthracene is the sole absorbing moiety at $\lambda_{exc} = 360$ nm, while at $\lambda_{exc} = 280$ nm the naphthalene moiety absorbs *ca.* 90% of the excitation light and anthracene less than 10%.

Inspection of Fig. 9 clearly shows that while selective excitation of the anthracene moiety leads to its own fluorescence emission, Fig. 9B, the 90% excitation of naphthalene moiety gives rise to an intense fluorescence emission from the anthracene, and only a



Scheme 8.



Scheme 9.

minor emission from naphthalene itself, Fig. 9C. This is what should be expected from an efficient energy transfer process. The energy transfer can be confirmed through the excitation spectrum collected at the anthracene emission (420 nm), Fig. 9A, where a large contribution from the naphthalene absorption is clear. The energy transfer (ET) parameters of this system have been calculated: the ET efficiency is $\eta = 0.94$, the Förster's critical distance is $R_0 = 28 \text{ \AA}$, and the inter-chromophoric distance for the fully protonated form, $R = 19 \text{ \AA}$.

The reductive quenching of hydrocarbon fluorophores by aliphatic amines can be used to control the energy transfer process. On this basis, it is possible to switch from energy transfer to electron transfer by increasing the pH or by metal ion coordination, as shown in Scheme 9. In the absence of protons or metal coordination, the electron transfer is the dominant process and no fluorescence emission can be observed. Protonation of the polyamine bridge or Zn^{2+} complexation prevents the electron transfer and allows the energy transfer to take place.

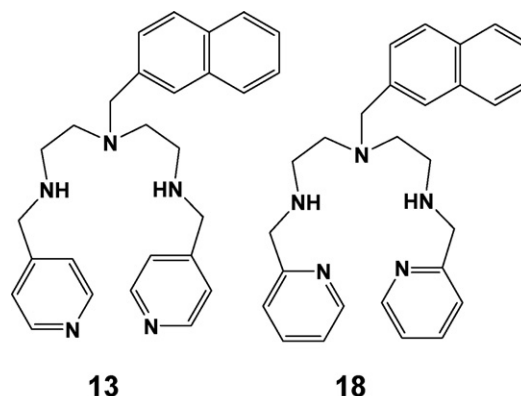
4. Receptor unit

In order to tune the receptor properties the incorporation of aromatic amines like pyridine or phenanthroline inside the cycles as in **11** or as appending units like in **13** has been explored. The introduction of aromatic amines not only completely modifies the ability of the ligand to complex metals, but also affects the characteristics of the fluorescence emission. One interesting example regards the Zn^{2+} complexes with compounds **13** and **18** (Scheme 10). In the case of the complex Zn13 , the plateau is very small, and the domain of this species is a sharp curve with maximum peak around pH 8.0 [30]. In contrast, the titration curve of complex Zn18 exhibits an extended plateau from 5 to 9 (see Fig. 10). This different behaviour can be explained by the participation of the pyridine units in the

binding. In compound **13**, these units present the nitrogen atoms in position 4, far from the polyamine chain, while in **18** the nitrogen atoms are located in position 2, and the stiffening effect observed in this compound is not present in compound **13**. The complex is much stronger and by consequence Zn18 is the dominant species in a large pH range. This fact is also reflected in the higher value of the stability constant of the Zn18 complex ($\log K = 13.0$) when compared with the analogue Zn13 complex ($\log K = 4.72$).

In compound Zn13 protonation of the pyridine units at moderately acidic values contribute to the quenching effect at these pH values, while in Zn18 the pyridines are involved in the binding with the metal and lower pH values are needed to obtain quenching.

This example illustrates the potentialities of the design in new receptors based on polyamines and the role that the introduction of other units in their structure can play to render more efficient the sensing of metal cations or other target molecules.



Scheme 10.

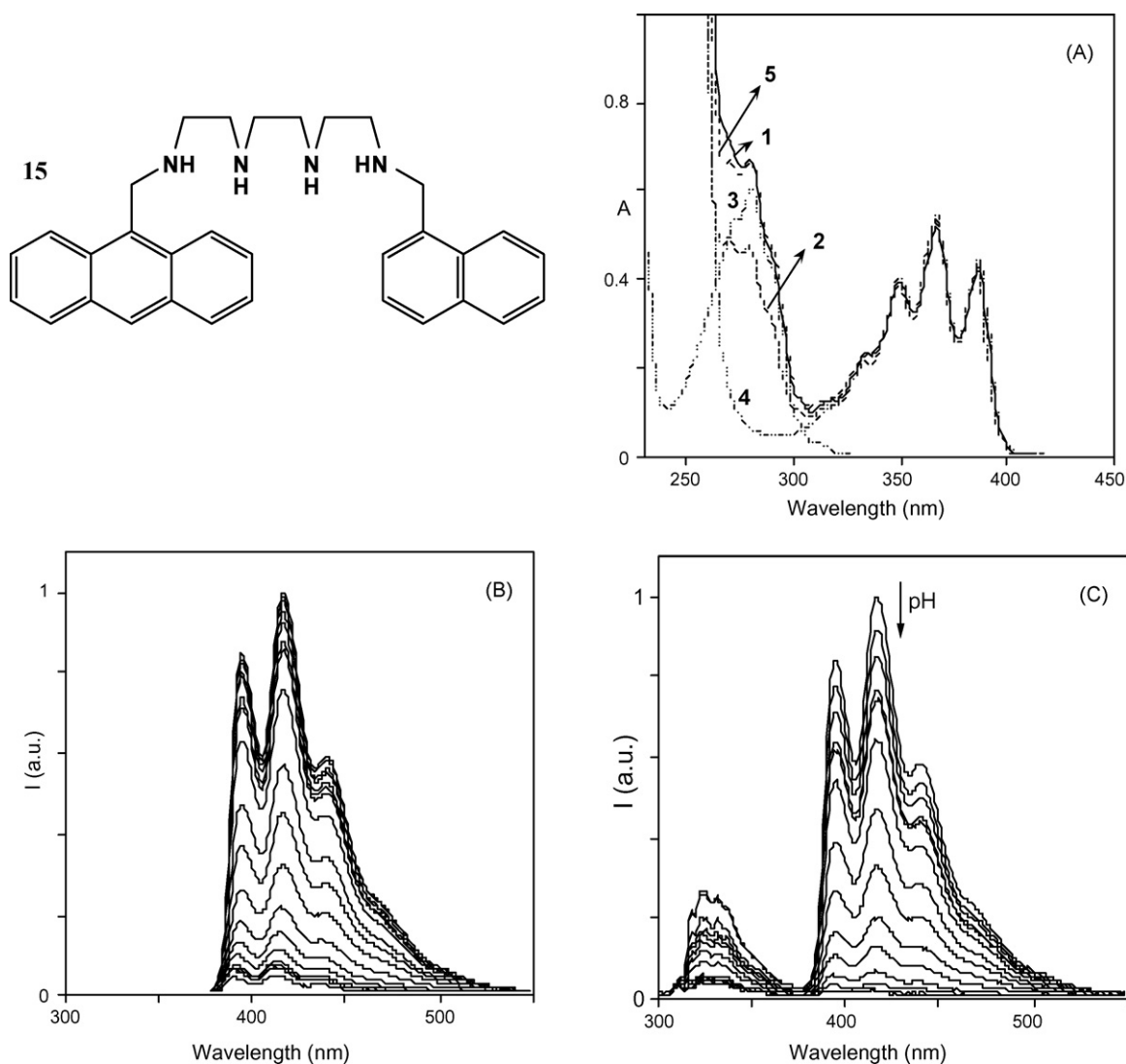


Fig. 9. (A) Absorption spectrum (1) and respective excitation spectrum at $\lambda_{em} = 420$ nm (2) of compound **15**; absorption spectrum of naphthalene derivative model compound **16** (3), absorption spectrum of anthracene model compound **17** (4), both in the same concentration as **17**, and the sum 3 + 4 (5) were represented for comparison purposes. (B) Fluorescence emission spectra upon selective excitation of anthracene at $\lambda_{exc} = 360$ nm. (C) Fluorescence emission spectrum upon excitation at $\lambda_{exc} = 280$ nm, 90% naphthalene excitation [33].

4.1. Phenanthroline, bipyridine and terpyridine units

Incorporating or appending phenanthroline, bipyridine or terpyridine units has been the subject of recent research by some authors [34]. In collaboration with the group of Bianchi and Bencini several examples of this strategy have been reported since 1999 [27,28,33,35]. In this case the aromatic amines can be used for both functions, binding and sensing.

In Scheme 11 a family of compounds having the phenanthroline incorporated into the polyamine macrocycle is shown [35]. The fluorescence emission of the free ligands presents the common trend of the compounds possessing both aromatic and aliphatic amines, a bell shape fluorescence emission titration curve. The quenching effect at lower pH values depends on the chain length and is more pronounced for $n=3$ as expected by the easier protonation of the phenanthroline for the larger macrocycles.

In the case of Zn^{2+} complexes of compound **19** ($n=1$) (Scheme 11) the benzylic nitrogen atoms are weakly bound to the metal, and for this reason no fluorescence emission is observed because the benzylic amines are available to the PET process of

quenching. On the other hand a decrease of the stability trend for the complexes with Zn^{2+} from $n=1$ to 3 was observed. This fact suggests that the number of donor atoms participating in the coordination does not parallel the increasing number of donors in the ligands. Moreover an increasing number of uncoordinated amine groups favours the formation of protonated complexes, as was observed for $n=2$ and $n=3$, and allows the larger ligand to have enough free donor atoms to bind a second metal [36]. In order to observe the fluorescence emission, the nitrogen atoms should be involved in the binding with the metal or protonated. This is in agreement with the observation that the largest fluorescence emission occurs for the diprotonated metal complex with $n=3$ ligand [36].

Similar behaviour was found more recently for the phenanthroline systems **20** and **21** (Scheme 12) [37].

While ligand **21** permits coordination of divalent metal ions such as Cu^{2+} , Zn^{2+} , Cd^{2+} , Pb^{2+} and Hg^{2+} given mononuclear complexes (see Hg^{2+} complex in Fig. 11), ligand **20** gave both mono- and dinuclear complexes [37]. The metal complexes with **20** and **21** do not display fluorescence emission, due to the presence of amine groups

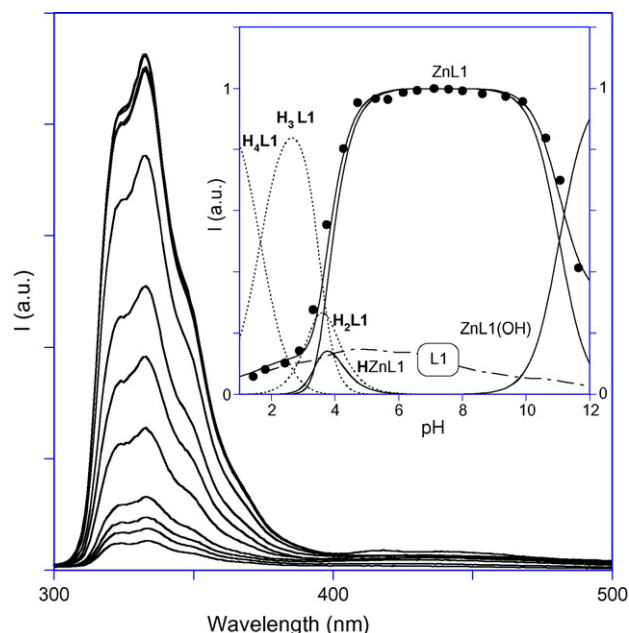
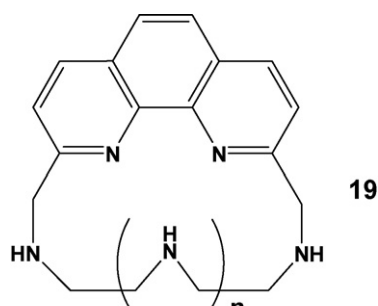
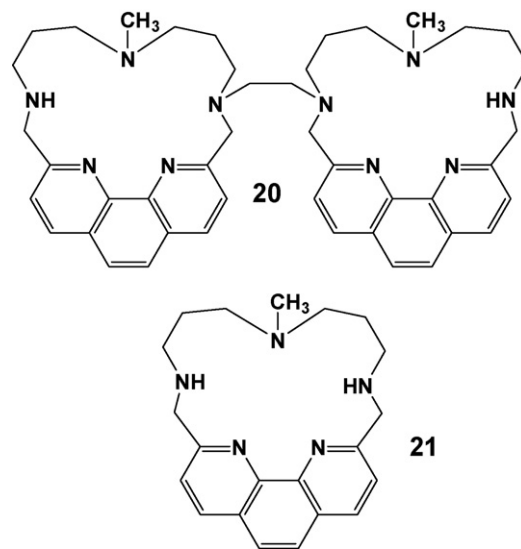
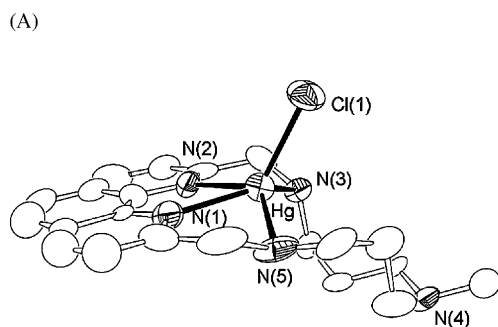


Fig. 10. Emission spectra of the complex Zn(**18**) as a function of pH ($\lambda_{\text{exc}} = 260$ nm, Zn(**18**) = 5.0×10^{-5} M, [NaCl] = 0.15 M). Inset: Fluorescence emission titration curve of the complex Zn(**18**) $^{2+}$ ($\lambda_{\text{exc}} = 260$ nm, $\lambda_{\text{em}} = 335$ nm (●), [Zn(**18**) $^{2+}$] = 5.0×10^{-5} M, [NaCl] = 0.15 M) superimposed on the respective mole fraction distribution of species. Traced line: relative fluorescence emission titration of the free ligand [31].



Scheme 11.



Scheme 12.

not involved in metal coordination. These amine groups quench the excited fluorophore through an electron transfer process.

The dinuclear Zn $^{2+}$ complex with **21** shows remarkable hydrolytic ability for bis-(*p*-nitrophenyl) phosphate (BNPP), due to the simultaneous presence within this complex of two metals and two hydrophobic units. In fact, the two Zn $^{2+}$ ions act cooperatively in substrate binding, probably through a bridging interaction of the phosphate ester; the interaction is further reinforced by π -stacking pairing and hydrophobic interactions between the phenanthroline unit(s) and the *p*-nitrophenyl groups of BNPP [37].

The chemosensor **22** bearing two naphthalene and two phenanthroline units was investigated in the presence of transition metals such as Cu $^{2+}$ and Zn $^{2+}$ (Fig. 12) [38]. The fluorescence emission spectra of **22** show the simultaneous presence of three bands: a short wavelength emission band (naphthalene monomer), a middle emission band (phenanthroline emission) in addition to a long-wavelength band. All three bands were found to be dependent on the protonation state of the macrocyclic unit (including the polyaminic and phenanthroline structures). The long wavelength emission was analysed in great detail and it was attributed to an intramolecular interaction between a ground state phenanthroline and an excited state phenanthroline, suggesting that phenanthro-

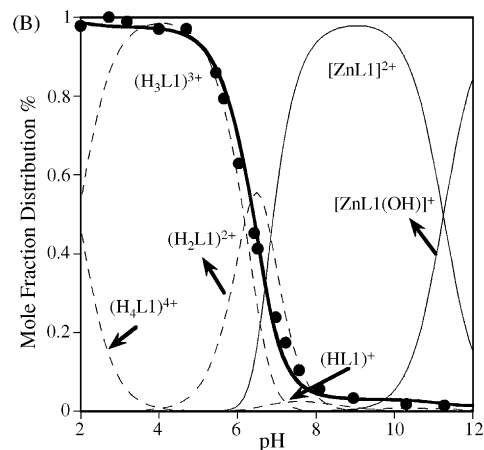


Fig. 11. (A) ORTEP drawing of the [H(**21**)HgCl] $^{2+}$ cation with the numbering scheme adopted (displacement ellipsoids drawn at 50% probability level); (B) Fluorescence emission at 366 nm (●) for the systems Zn(II)/(**21**) superimposed to the corresponding distribution diagrams ($\lambda_{\text{exc}} = 272$ nm, [Zn(II)] = [L1] = 1.31×10^{-5} M; $I = 0.1$ M NMe $_4$ Cl, 298 K). Distribution curves of the complexed species represented as solid line, protonated species as dotted lines [37].

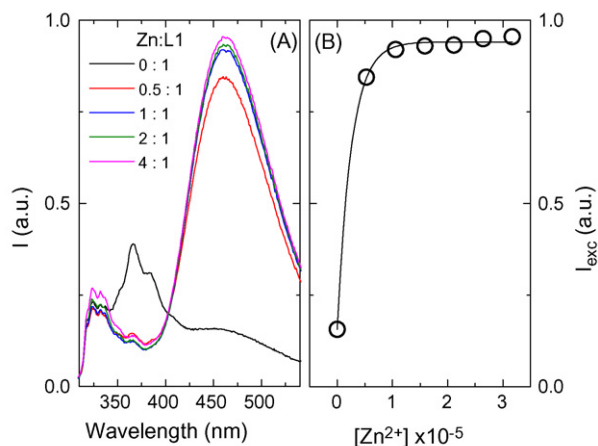
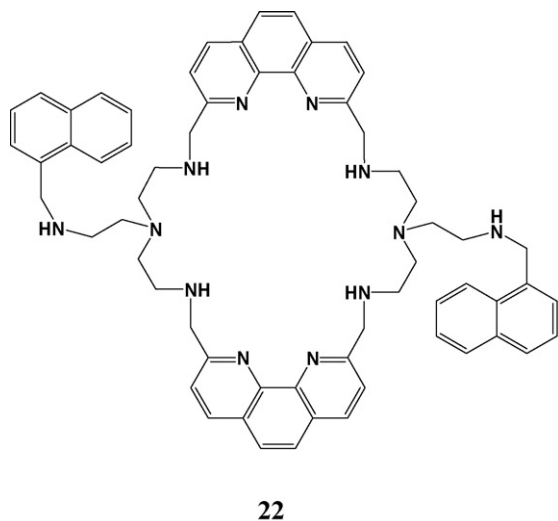


Fig. 12. (A) Variation of the fluorescence emission spectra with added Zn^{2+} presented for molar ratios of $\text{Zn}(\mathbf{22})$ varying from zero:one to 4:1 of $\text{Zn}^{2+}(\mathbf{22})$ and (B) presentation of the variation of the excimer intensity maximum (obtained at 460 nm) with Zn^{2+} for $[\mathbf{22}] = 1 \times 10^{-5}$ M. The excitation wavelength was 275 nm [38].

line can give rise to excimer emissions [38]. The excimer formation is dramatically increased in the presence of Zn^{2+} and decreased with Cu^{2+} (see Fig. 12 for Zn^{2+}). It is shown that depending on the metal the long-emission band presents a different wavelength maximum, which can be considered as a characteristic to validate the ligand **22** as a sensor for a given and specific metal.

Concerning the bipyridine system, the fluorescence emission of compounds **23** and **24** was reported (Fig. 13) [39]. In the first compound the disposition of the heteroaromatic and aliphatic nitrogen donors is convergent toward the macrocyclic cavity, while in the second two aromatic nitrogen atoms point outside the cavity.

A crystal structure of this last compound (Fig. 13) shows two well-separated binding zones, the macrocycle cavity and the

external dipyridine units. In the case of the mononuclear complexes with Zn^{2+} and compound **23** the crystal structure of $\text{Zn}(\mathbf{23})$ (Fig. 13) indicates that the metal is coordinated inside the cavity bound to the heteroaromatic nitrogen donors and to the three amines of the aliphatic chain. The benzilic nitrogen atoms are not involved in the bonding, facile protonation of these two nitrogen atoms takes place at acidic pH values and by consequence this species is the one exhibiting the largest fluorescence emission. In the case of the mononuclear Zn^{2+} complex of compound **24**, the metal is encapsulated inside the cavity, not coordinated by the dipyridine unit. Protonation of the complex occurs on the aliphatic polyamine chain and gives rise to the translocation of the metal outside the cavity, bound to the heteroaromatic nitrogen atoms (Fig. 14).

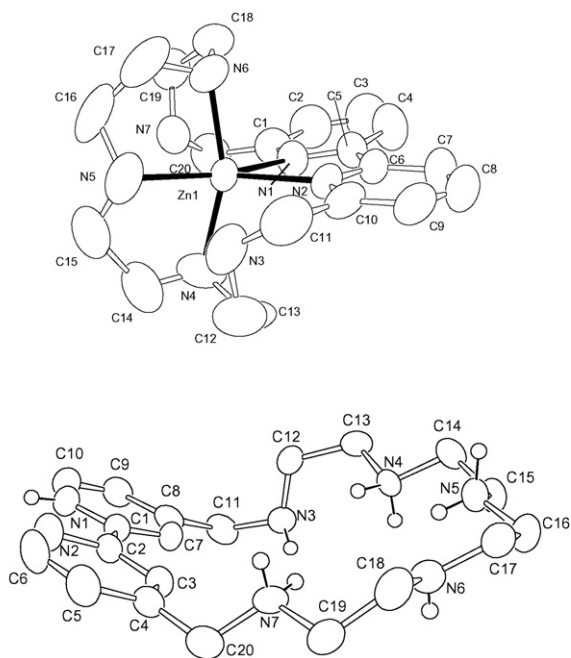
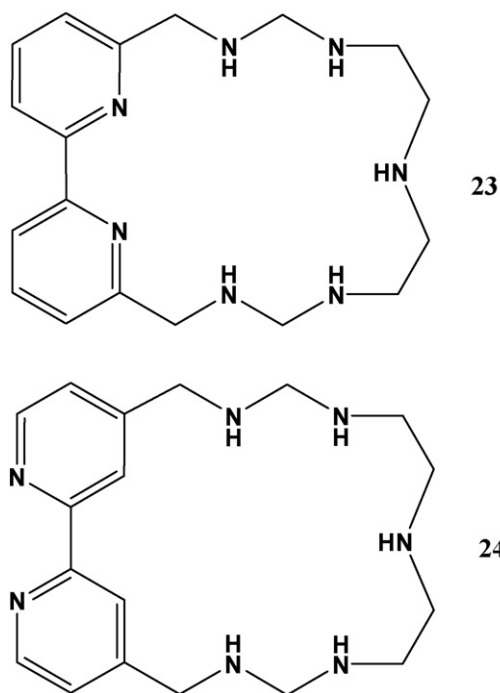


Fig. 13. ORTEP drawing of the $[\text{Zn}\mathbf{23}]^{2+}$ and $[\text{H}_4\mathbf{24}]^{4+}$ cation [39].

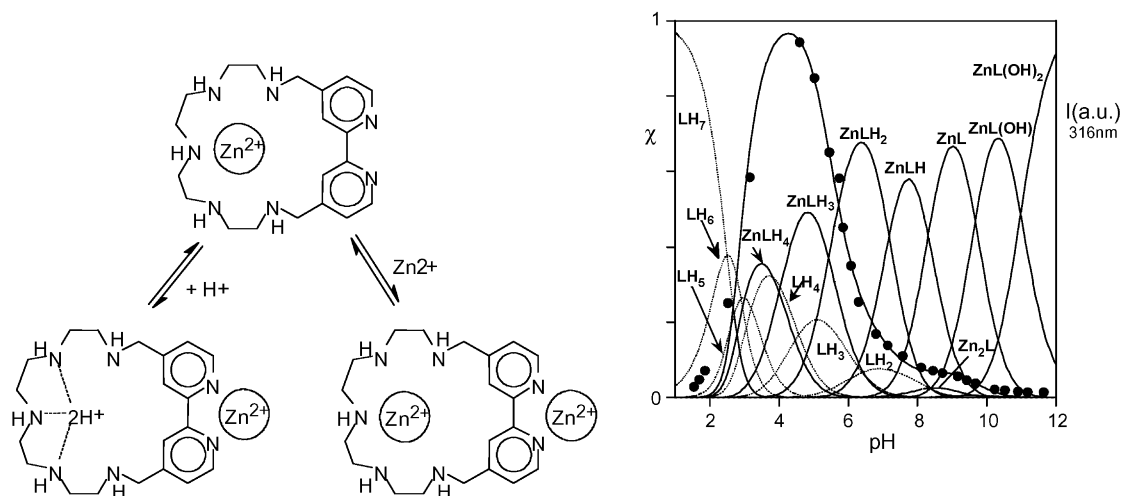


Fig. 14. Schematic representation on the metal jumping from inside to outside and fluorescence emission (●) and molar fractions of the protonated and complexed species of **24** (dashed lines) in the presence of Zn^{2+} (1:1 molar ratio) as a function of pH ($[\text{24}] = 2.5 \times 10^{-5} \text{ M}$; $I = 0.1 \text{ M}$). Charges of the complexes are omitted for clarity [39].

Similar effects have been also reported for Cu^{2+} and Ni^{2+} with macrocycle **24**, but in both cases a non-emissive species was observed [40].

Macrocycle **25** containing a terpyridine unit was reported (see Fig. 15) [41]. A potentiometric, ^1H NMR, UV–vis spectrophotometric and fluorescence emission study on the basicity properties of **25** in aqueous solutions is compatible with the first four protonation steps occurring on the polyamine chain, while the terpyridine nitrogen atoms are involved in proton binding only in the last protonation step at strongly acidic pH values. Mono- and dinuclear complexes with Cu^{2+} , Zn^{2+} , Cd^{2+} and Pb^{2+} are formed in solution. Cu^{2+} and Zn^{2+} can form both mono- and dinuclear complexes in solution, while the larger Cd^{2+} and Pb^{2+} give only mononuclear complexes. In the $[\text{M}(\text{25})]^{2+}$ complexes ($\text{M} = \text{Zn}^{2+}$ or Cd^{2+}) the metal is unequivocally bound to the terpyridine unit. Crystal structures were obtained and show two $[\text{M}(\text{25})\text{H}]^{3+}$ units coupled by a bridg-

ing OH^- or Br^- anion (See Fig. 15). A π -stacking interaction between the terpyridine moieties helps to stabilize the complexes. A potentiometric and spectrophotometric study shows that, in the case of Cu^{2+} and Zn^{2+} , the dimeric assemblies are also formed in aqueous solution containing the ligand and the metals in 1:1 molar ratio. Protonation of the complexes or addition of a second metal ion leads to disruption of the dimers, due to the increased electrostatic repulsions between the two monomeric units [41].

The fluorescence emission of compound **25** is also strongly affected by metal coordination. Fig. 16 reports the pH dependence of the fluorescence emission spectra recorded on solutions containing the ligand and $\text{Zn}(\text{II})$ in 1:1 molar ratio. Comparison of the fluorescence emission intensity of the ligand **25** in the absence and in the presence of Zn^{2+} (Fig. 16B) clearly shows an increase of the fluorescence emission in the presence of the metal in the acidic pH region, where the $[\text{Zn}(\text{25})\text{H}_3]^{5+}$ complex is formed. A

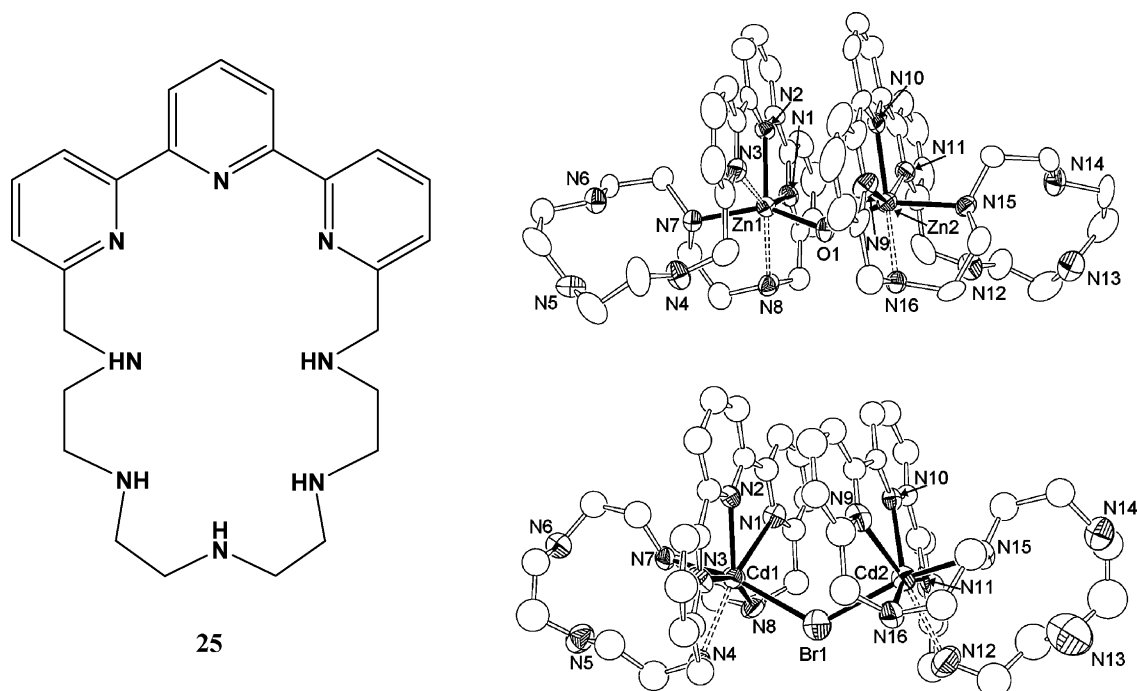


Fig. 15. ORTEP drawing of the $\{[\text{Zn}(\text{25})\text{H}]_2(\mu\text{-OH})\}^{5+}$ and $\{[\text{Cd}(\text{25})\text{H}]_2(\mu\text{-Br})\}^{5+}$ cation [41].

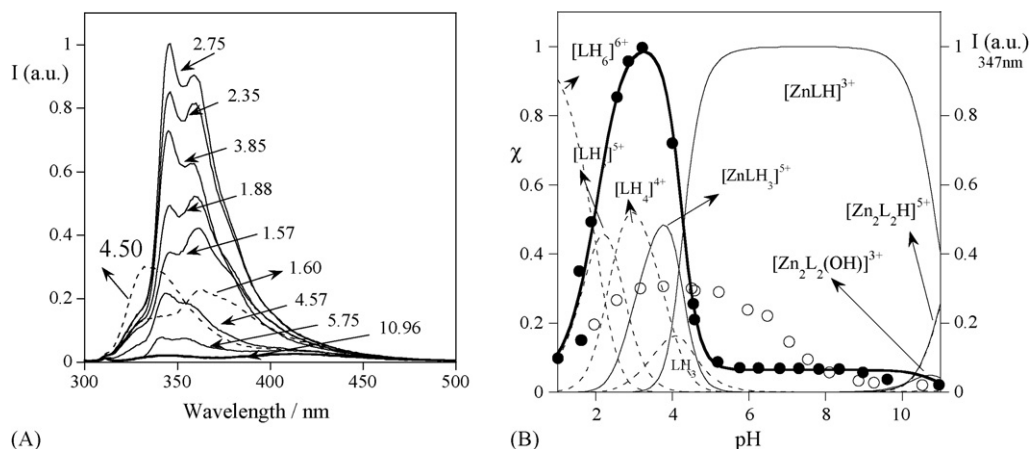


Fig. 16. (A) Fluorescence emission spectra of the Zn^{2+} complexes with **25** at different pH values (excitation wavelength of 282 nm). (B) Fluorescence emission at 347 nm of **25** in the absence (\circ) and in the presence of Zn^{2+} (1:1 molar ratio) (\bullet) and molar fractions of the protonated (dashed lines) and complexed species of **25** as a function of pH ($[\text{25}] = 2.82 \times 10^{-5} \text{ M}$; $I = 0.1 \text{ M NMe}_4\text{Cl}$). Charges of the complexes are omitted for clarity [41].

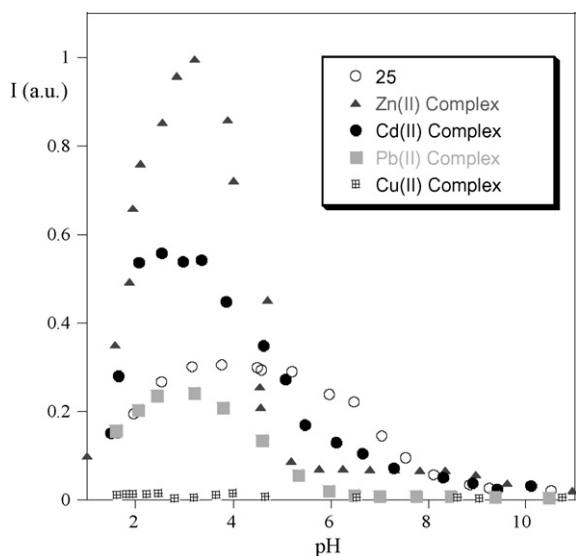


Fig. 17. Fluorescence emission at 347 nm of **25** and its Zn^{2+} , Cd^{2+} , Pb^{2+} and Cu^{2+} complexes (1:1 molar ratio) as a function of pH ($[\text{25}] = 2.82 \times 10^{-5} \text{ M}$; $I = 0.1 \text{ M NMe}_4\text{Cl}$) [41].

similar behaviour is also found in the case of Cd^{2+} , where only the $[\text{Cd}(\text{25})\text{H}_2]^{4+}$ complex is emissive. The fluorescence emission titration curves for this ligand and in the presence of Zn^{2+} , Cd^{2+} , Cu^{2+} and Pb^{2+} (metal to ligand 1:1 molar ratio) are summarized in Fig. 17.

5. Applications

5.1. Exploring the photocatalytic properties

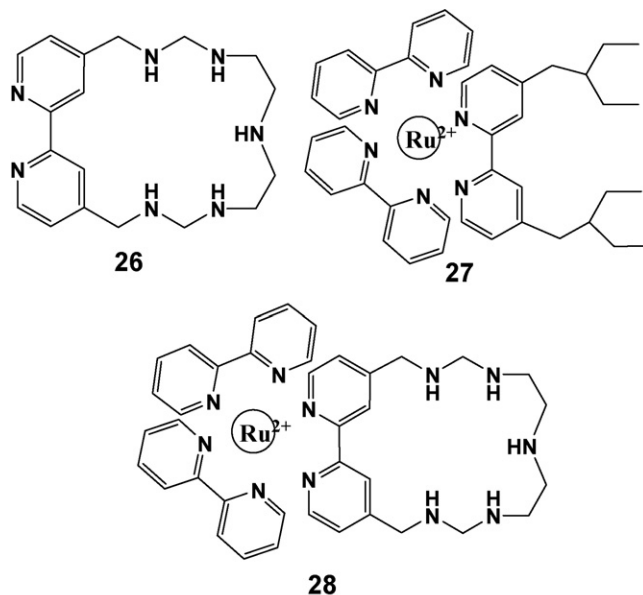
Macrocycles containing endotopic cavities and exotopic coordination sites can be used as ligands in the construction of water-soluble fluorescent metal complexes, see Scheme 13. These coordination compounds can operate as luminescence chemosensors based on the emission intensity as well as in long lifetime-based sensing for cations and anions. The particular usefulness of lifetime based sensing systems has been pointed out, by Lakowicz [42,43], see compound **27**, essentially because they do not depend on probe concentration and remain unaffected by the photobleaching or washout of the probe. Compound **28** was

synthesized taking profit of an exotopic macrocycle compound **26** [39].

As could be expected, coordination ability of **28** towards Zn^{2+} and Cu^{2+} is reduced in comparison with the parent ligand **26** due to the electrostatic repulsion brought by the ruthenium. The absorption and emission of the mononuclear Zn^{2+} complexes with **28** is only slightly red-shifted relative to the non-complexed compound **26**. While Cu^{2+} is also able to form dinuclear species the ligand does not display a great tendency to bind the second metal. In this case the emission shows a dramatic quenching upon coordination to the metal. The quenching of the emission of $[\text{Ru}(\text{bpy})_3]^{2+}$ by polyamine complexes of Cu^{2+} ion was previously described by Moore and Alcock and attributed to energy transfer from the excited state of $[\text{Ru}(\text{bpy})_3]^{2+}$ to the copper complex, promoting a d–d transition of Cu^{2+} [44].

An interesting effect is the possibility of exploring the cavity as a photocatalytic center capable to host substrates amenable to react upon electron or energy transfer involving the metal center [45].

An example of this photocatalytic effect is the adduct formed between compound **28** and iodide (see Fig. 18) [45].



Scheme 13.

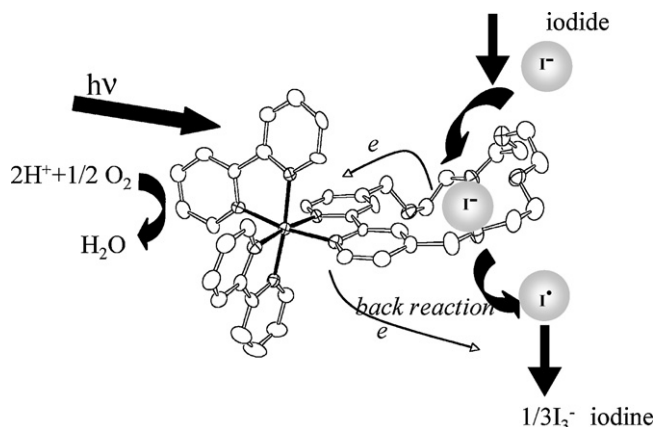
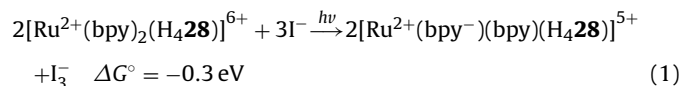


Fig. 18. Photocatalytic cycle for the oxidation of iodide to iodine by dioxygen [45].

Excitation of compound **28** in the MLCT band allows the transfer of one electron from I^- to the Ru^{2+} complex, leading to the formation of an iodine radical and reduced Ru^{2+} complex (the electron goes to one of the bpy moieties). The iodine radical gives I_3^- as a final product by a sequence of well-known reactions [46]. The cycle is completed by reoxidation of the reduced bpy moiety of the complex by dioxygen.

As proven by the inertness of the parent compound $[Ru(bpy)_3]^{2+}$, the existence of the positively charged macrocyclic receptor seems to be an indispensable requirement to fix the iodide in a position close to the metal, in order to allow the electron transfer process. In the case of $H_4\mathbf{28}^{6+}$, the net reaction can be accounted in Eq. (1) which is thermodynamically favourable by 0.3 eV.



The relatively low efficiency of this system (0.35 in solution saturated with dioxygen) can be attributed to the fact that only 5% of the excited state can be quenched by iodide. In addition there is evidence, from preliminary flash photolysis experiments, that the back reaction from the reduced Ru^+ complex to I_3^- is a competitive process that decreases the net formation of photoproducts.

5.2. Sensing anions

It is well known that macrocyclic polyamines in their protonated forms are efficient receptors of anionic species in solution [46]. In particular very stable adducts are formed with $[Fe(CN)_6]^{4-}$ and $[Fe(CN)_6]^{3-}$, principally due to the high negative charge of such anions [47–51]. Protonated species of compound **28** might be able to form similar adducts. Our principal interest towards such systems results from the fact that the emission of the parent compound $[Ru(bpy)_3]^{2+}$ is known to be efficiently quenched by electron

transfer from (or to) metal-cyanide complexes [52,53], and thus $[Ru(bpy)_3]^{2+}$ could be used as sensor for this type of anions. Compound **28** contains the basic ruthenium sensing unit, but in addition possesses an extra binding polyamine receptor, that is expected to influence the overall process, improving the efficiency in anion sensing. The interaction between compound **28** with $[Fe(CN)_6]^{4-}$ and $[Fe(CN)_6]^{3-}$, was studied on the basis of the Stern-Volmer plots of the intensity (I_0/I) and lifetimes (τ_0/τ) and compared with the behaviour of $[Ru(bpy)_3]^{2+}$, in identical conditions, the results being summarized in Table 2. The studies were carried out at pH 4 and at this pH value the polyamine of compound **28** exhibits 4 protons ($H_4\mathbf{28}$).

The ion-pair association is negligible for the pair between $[Ru(bpy)_3]^{2+}$ and $[Fe(CN)_6]^{3-}$ and in the case of the pair $[Ru(bpy)_3]^{2+}$ and $[Fe(CN)_6]^{4-}$, I_0/I is somewhat higher than τ_0/τ , allowing one to calculate an ion-pairing association $K_{ip} < 300 \text{ M}^{-1}$. This implies that the quenching process is essentially dynamic in both cases, see Fig. 19A and B. On the other hand, in the case of compound **28**, there is a great component of static quenching that is brought about by the extra charge of the polyamine (Fig. 19A and B).

An interesting example of anions sensing was reported for compound **11** (Scheme 6). Among the Krebs cycle components, just citrate enhances the fluorescence this compound, see Fig. 20 [54].

The main species responsible for the enhanced of the emission of compound **11** in the presence of citrate are $H_6(\mathbf{11})A^{2+}$ and $H_5(\mathbf{11})A^{2+}$ (A = citrate) and it was shown that citrate is the anion best suited for forming hydrogen bonds with the arms of compound **11** thus enhancing the fluorescence.

Interaction of ATP, ADP and AMP was also reported a few years ago for compound **6** and similar species bearing a naphthalene or anthracene sensing units attached to a polyamine chain [55].

5.3. Antenna effect

The photophysical properties of the $Eu(III)$, $Tb(III)$ and $Ru(II)$ complexes with dipyrindine containing cryptands, such as compound **30** (Fig. 21), have been extensively studied in the past few years [56–58].

Encapsulation of Eu^{3+} inside the cryptand cavity allows one to overcome the drawback of the extremely low absorption coefficient of the un-complexed metal, the so-called antenna effect. Cryptands are capable not only of efficiently binding the metal, but also to protect it from the solvent, especially in aqueous solution where coordinated water is an efficient quencher of the emission.

Compound **29** was synthesized in order to contain a coordinative cleft as potential binding site for metals [59]. However, the most significant difference from previously reported cryptands, such as compound **30**, is the presence of an aliphatic polyamine chain which can easily bind protons in aqueous solutions. These structural features make compound **29** an appropriate ligand for simultaneous Eu^{3+} and H^+ binding. Indeed, the diprotonated

Table 2

Association constants ($\log K_{ip}$) and quenching rate constants (k_q) determined from photophysical quenching studies [41].

	$\log K_{ip}$	$K_{SV} (\text{M}^{-1a})$	$K_{SV} (\text{M}^{-1b})$	$k_q (\text{s}^{-1} \text{M}^{-1})$
$[Fe(CN)_6]^{4-} + [Ru(bpy)_3]^{2+}$	≤ 2.5	2325	1358	5.8×10^{9c}
$[Fe(CN)_6]^{3-} + [Ru(bpy)_3]^{2+}$	–	3488	3310	8.7×10^{9c}
$[Fe(CN)_6]^{4-} + [Ru(bpy)_2(H_4\mathbf{28})]^{6+}$	4.7	4164	–	1.4×10^{10d}
$[Fe(CN)_6]^{3-} + [Ru(bpy)_2(H_4\mathbf{28})]^{6+}$	3.3	3697	–	1.3×10^{10d}

^a [41].

^b [47c]. All the experiments were carried out at 25 °C and air atmosphere at pH 4.0.

^c $\tau_0 ([Ru(bpy)_3]^{2+}) = 400 \text{ ns}$.

^d $\tau_0 ([Ru(bpy)_2(H_4\mathbf{28})]^{6+}) = 290 \text{ ns}$.

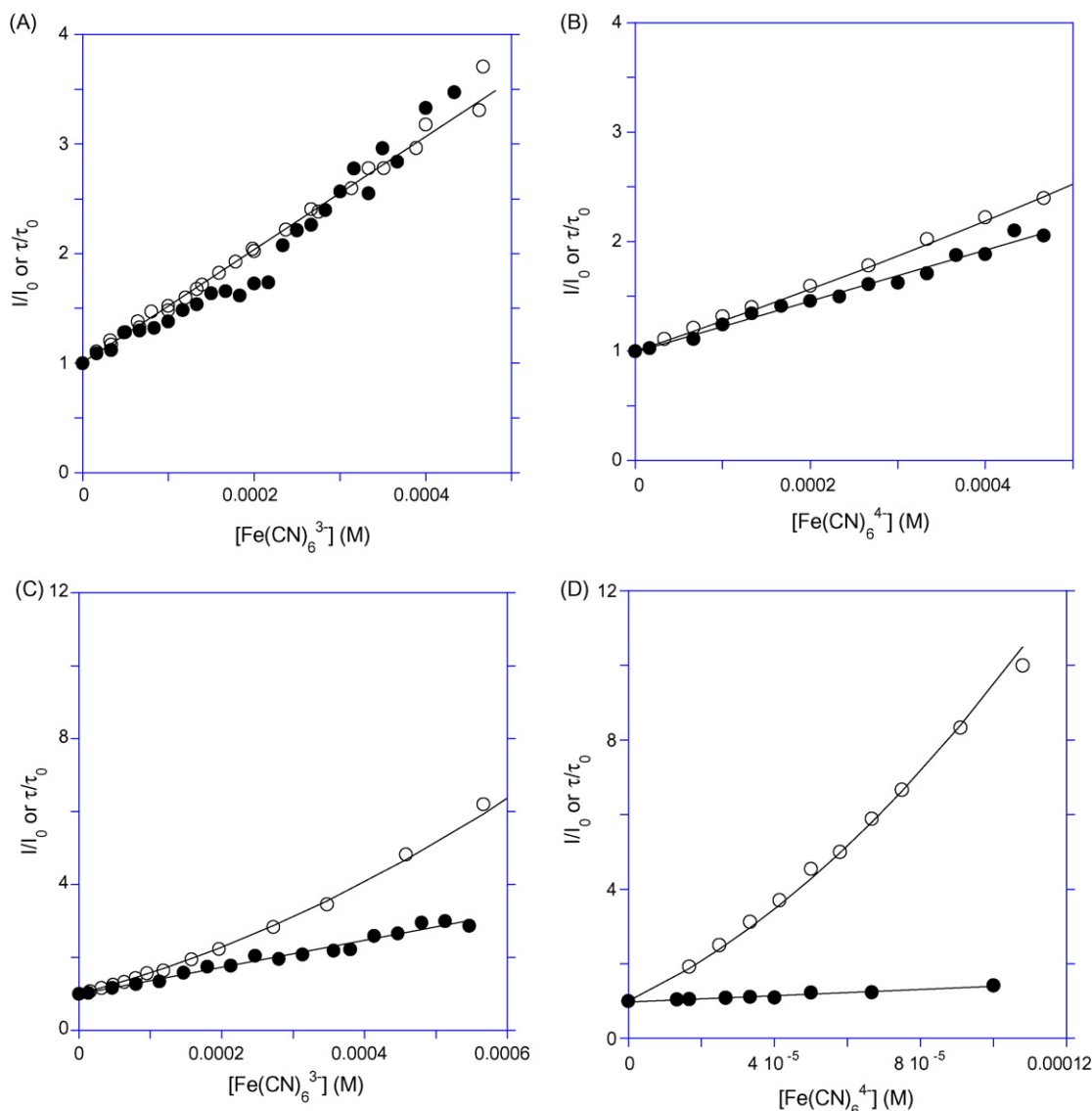


Fig. 19. Fluorescence intensities (○) and decay times (●) of: $[\text{Ru}(\text{bpy})_3]^{2+}$ (A and B) and **28** in the $\text{H}_4\text{28}^{6+}$ form (C and D) with $[\text{Fe}(\text{CN})_6]^{3-}$ and $[\text{Fe}(\text{CN})_6]^{4-}$ at pH 4.0. All the experiments were carried out at 25 °C and air atmosphere [45].

complex $[\text{EuCl}_2\text{H}_2(\text{29})](\text{ClO}_4)_2 \cdot 4\text{H}_2\text{O}$ crystallizes from aqueous solutions at acidic pH's containing **29** and Eu^{3+} (see Fig. 21).

In this structure the polyamine chain is weakly involved in metal coordination and can easily be protonated. Moreover, water molecules may reasonably replace these anions in aqueous solutions in the absence of chloride.

As expected, the luminescence spectrum of the $\text{Eu}(\text{III})$ cryptate in aqueous solution at pH 6.8, in the absence of chloride, shows the characteristic visible emission of the metal with a maximum at 617 nm, upon excitation at 306 nm. The emission from the metal upon excitation of the ligand was previously observed for many other $\text{Eu}(\text{III})$ cryptate complexes. As mentioned above, the lanthanide(III) metal presents very low molar absorption coefficients and thus the excitation light is almost exclusively absorbed by the ligand. The observed emission from Eu^{3+} can thus be explained by an intramolecular energy transfer to the metal ion mainly from the higher energy triplet state of the cryptand. Fig. 22A shows the fluorescence emission spectra of the cryptate at different pH values, while Fig. 22B reports the titration curve obtained by following the fluorescence emission at 617 nm. The results can be explained hav-

ing in mind that the three central nitrogen atoms of the polyamine chain show a high tendency to bind protons.

The first three constants correspond to protonation of the three not-coordinated amine groups of compound **29** to give the $[\text{EuH}_n\text{29}]^{(n+3)+}$ ($n = 1-3$) complexes at acidic pH's, while the last two may be attributed to the formation of the hydroxylated $[\text{Eu}(\text{OH})_2\text{29}]^{2+}$ and $[\text{Eu}(\text{OH})_2\text{29}]^+$ complexes at alkaline pH's. Protonation of the aliphatic polyamine chain $\text{N}2'/\text{N}1/\text{N}2$ prevents the interaction of the methylated amine groups with the metal. Therefore, the metal core is less protected from the solvent molecules. The free binding sites are occupied by water molecules, which can act as effective quencher of the luminescence. This hypothesis is confirmed by the analysis of the lifetimes of the cryptate complex in water at neutral and acidic pH's [60]. Applying the Horrocks and Sudnick equation [61], to these data, it can be estimated that *ca.* two water molecules are coordinated to the metal at pH 2 and just one at pH 6.8 [62]. The increasing number of coordinated water molecules at acidic pH values leads to a decrease of the luminescence emission. On the other hand, the observed decrease of the luminescence at alkaline pH values can be related to the formation

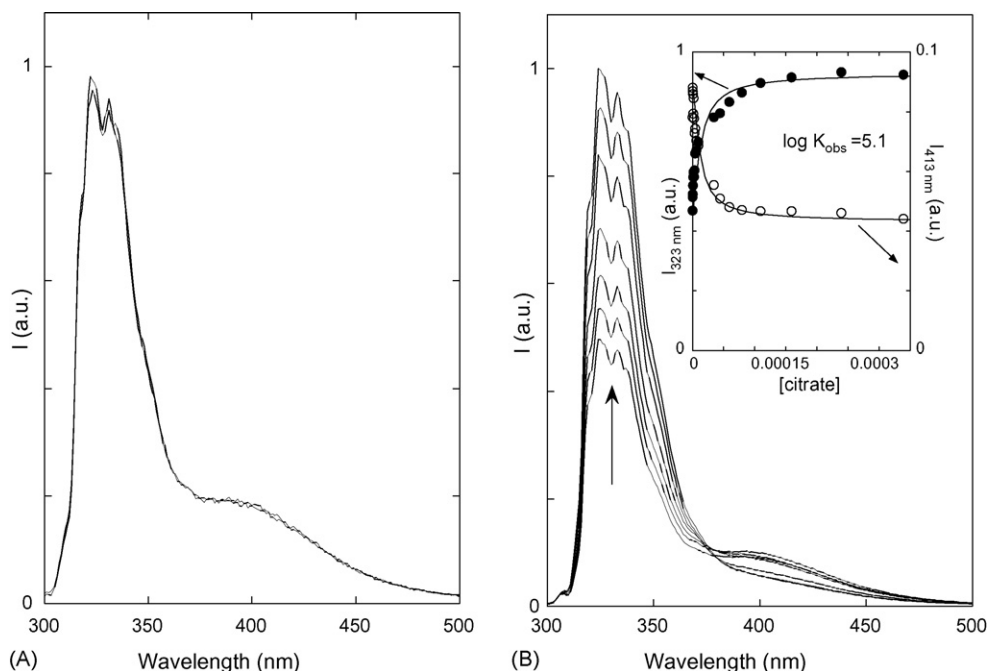


Fig. 20. (A) Fluorescence emission spectra of chemosensor (**11**), 1×10^{-5} M, in water at pH 5.8. The spectra in the absence and presence of isocitrate 3×10^{-4} M, are coincident; (B) the same in the presence of increasing quantities of citrate [54].

of the hydroxylated complexes $[\text{Eu}(\text{OH})_2\mathbf{29}]^{2+}$ and $[\text{Eu}(\text{OH})_2\mathbf{29}]^+$. Binding of hydroxide anions to Eu(III), in fact, usually give rise to a quenching of the emission.

The quantum yield in aqueous solution at pH 6.8 ($\Phi = 0.014$ at 300 K), the radiative rate constant ($k_r = 746 \text{ s}^{-1}$), the non-radiative temperature independent rate constant ($k_{nr}(\text{OH}) = 1177 \text{ s}^{-1}$), and the temperature-dependent decay rate constant ($k_{nr}(T) \cong 0$), are similar to those reported for other bipyridine-containing europium cryptates [58] and somewhat lower than those found for $[\text{Eu}\mathbf{30}]^{3+}$ [61], as expected considering the replacement of a bipyridine chromophore unit of **30** by an aliphatic polyamine chain in **29**. The present complex, therefore, still remains an efficient luminescent system, but, at the same time, displays a peculiar feature, which is the pH dependence of the luminescence intensity, with a maximum at neutral pH.

5.4. Sensing ATP by metal complexes

Nucleotide recognition and sensing in water is an important challenge in supramolecular chemistry due to its many biological implications. One of the most important is the ATP because plays a basic role in the bioenergetics of all living organisms, the center for chemical energy storage and transfer being its triphosphate chain. As a consequence, many papers have been published regarding the interaction of ATP with abiotic systems; in particular those with polyamine-based sensors were described above [63].

In Nature, ATPases hydrolyzed ATP only in the presence of softer metal cations such as Ca^{2+} , Mg^{2+} , and Zn^{2+} . The metal is involved in the catalytic mechanism, acting as binding site for ATP or as cofactor, favouring the phosphoryl transfer process [64].

Using as chemosensor the mononuclear Zn^{2+} complex with ligand **25**, where the metal is bound to the terpyridine nitrogen atoms,

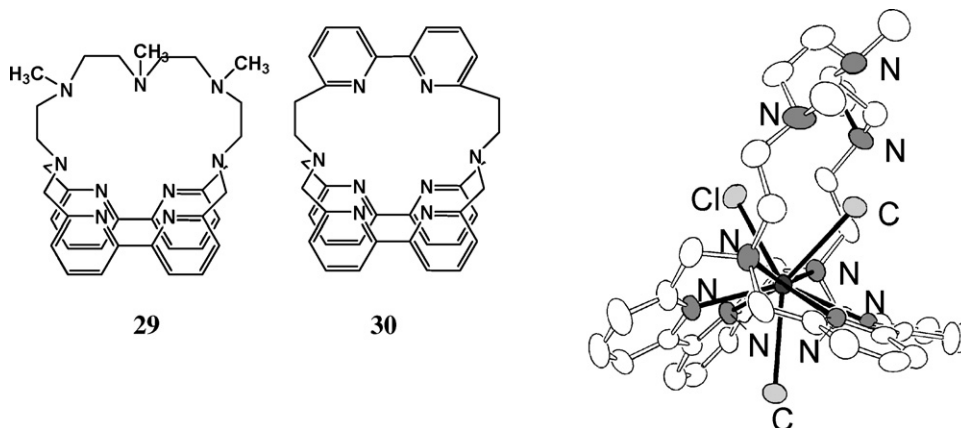


Fig. 21. Ligands **29** and **30**, and crystal structure of the $[\text{EuCl}_3\text{H}_2(\mathbf{29})]^{2+}$ cation [59,60].

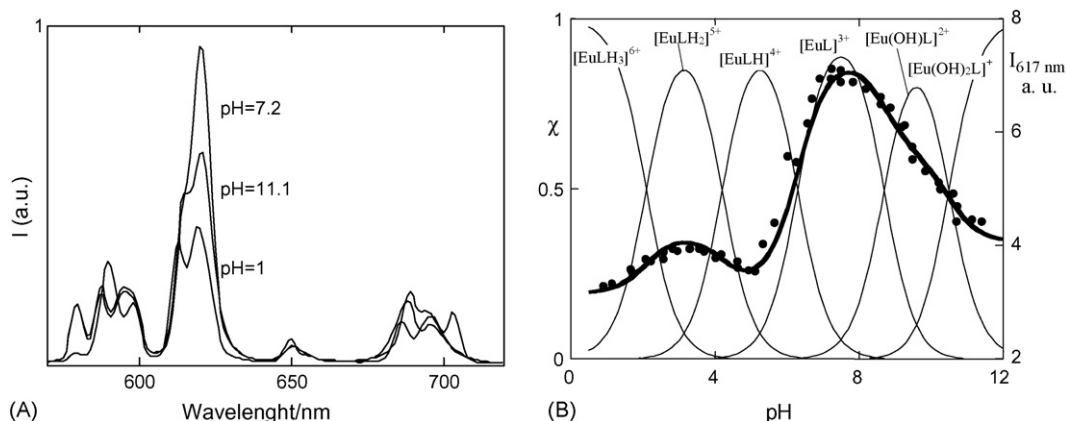


Fig. 22. (A) Fluorescence emission spectra of the europium cryptate complex in aqueous solutions at pH 1, 7.2 and 11.1. (B) Luminescence emission (●) of the Eu^{3+} complex with **29** ($\lambda_{\text{exc}} = 260 \text{ nm}$; $\lambda_{\text{em}} = 617 \text{ nm}$, $[\text{29}] = [\text{Eu}^{3+}] = 5 \times 10^{-5} \text{ M}$, $T = 300 \text{ K}$) and calculated molar fractions (χ) of the $\text{Eu}(\text{III})$ complexes (—) as a function of pH [59].

while the polyamine chain is not involved or weakly involved in metal binding and can easily be protonated in aqueous solutions to give $[\text{Zn}(\text{25})\text{H}_x]^{2+x}$ complexes [41], a second Zn^{2+} ion, can be coordinated affording dinuclear complexes [65].

The protonated $[\text{Zn}(\text{25})\text{H}_x]^{2+x}$ complexes, therefore, behave as multifunctional receptors for ATP, due to the simultaneous presence of metal-donor bonds, electrostatic and hydrogen bonding interactions and π -stacking pairing. The potentiometric study of this system shows that the Zn^{2+} complexes with **25** display a markedly higher affinity for ATP than the simple protonated species of the ligand **25** alone, confirming the crucial role of Zn^{2+} in ATP binding. The mononuclear Zn^{2+} complexes, however, do not show any significant ability in ATP hydrolysis. Addition of an equivalent of Zn^{2+} ion to solutions containing the mononuclear ternary complexes with ATP leads to the formation of dinuclear $\text{Zn}(\text{II})$ complexes with the nucleotide (see Fig. 23). The second metal ion is coordinated to the polyamine chain competing with protonation of the aliphatic amine groups. At this point, a fast cleavage process is observed by ^{31}P NMR at pH 4, where the $[\text{Zn}(\text{25})\text{H}_4\text{ATP}]^{2+}$ complex and the free Zn^{2+} are coexisting in solution (see Fig. 23).

The rate constants observed for the process $\text{ATP} \rightarrow \text{PN} + \text{ADP}$ fit the distribution curve of the tetraprotonated $[\text{Zn}(\text{25})\text{H}_4\text{ATP}]^{2+}$ species, with a maximum at pH 4 ($k_{\text{OBS}} = 3.2 \times 10^{-2} \text{ min}^{-1}$), thus indicating that this complex is the active species (see Fig. 23).

At pH 4, the phosphoramidate intermediate is formed, together with ADP, in the first few minutes up to a relatively high percentage (30%), compared with other polyammonium receptors able to hydrolyze ATP.

The present system $[\text{Zn}(\text{25})\text{H}_4\text{ATP}]^{2+}$, therefore, represents a unique case of ATP dephosphorylation promoted by the simultaneous action of a Zn^{2+} complex, which is used essentially for substrate

anchoring, and of a second metal, which acts as cofactor, assisting the phosphoryl transfer from ATP to an amine group of the receptor.

6. Oxa-aza-based receptors: Schiff-base and amine ligands with N_xO_y donor sets

In order to confer more “hard” properties to the receptor and increase the leak of metal ions to be complexed and detected, profit was taken from the introduction of oxygen atoms in the polyamine chain [66]. This strategy has however a drawback of render the chemosensor less soluble in water and as a consequence some of the systems reported in this section were studied in organic solvents or mixtures of water/organic solvents.

In collaboration with Bastida the synthesis of a comprehensive family of macrocyclic ligands (see Scheme 14) designed for metal complexation have been reported [67], and their interaction with lanthanide(III), transition metal ions, such as Cu^{2+} , Ni^{2+} , Co^{2+} , Mn^{2+} , post-transition metals Zn^{2+} , Cd^{2+} and the alkaline-earth Ca^{2+} were explored. In particular mono- and dinuclear complexes with ligands **31–37** were reported. No fluorescence emission was detected from these ligands [13–17].

Reduction of the double $\text{C}=\text{N}$ imine bonds to a $\text{C}-\text{NH}$ amine bond, leads to more flexible structures, see Scheme 15, and in some cases in the appearance of emissive properties. Similarly to that observed for the polyamine receptors, in these amine derivative systems, protonation of the nitrogen atoms is a necessary requirement to observe the fluorescence. However the fully protonated form is not the most emissive species due to the non-radiative decay involving a hydrogen bond between the oxygen atoms and the protonated benzylic nitrogen atoms. For example, if only one amine nitrogen atom is protonated in the solid state of compound

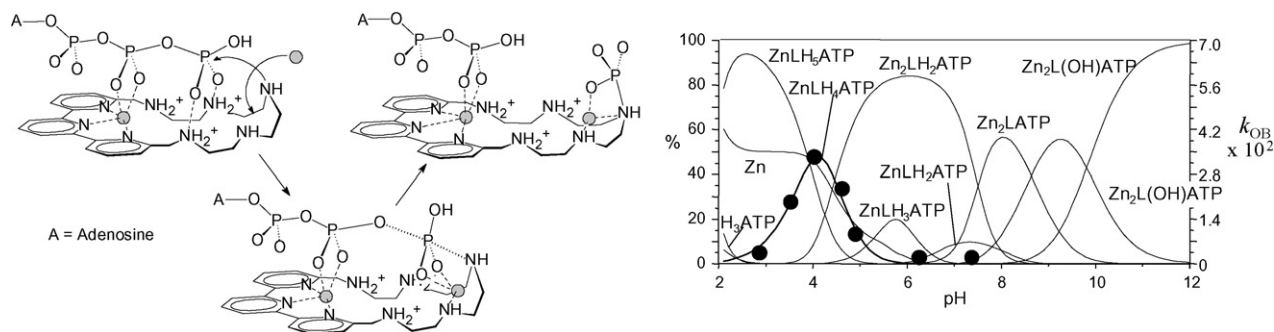
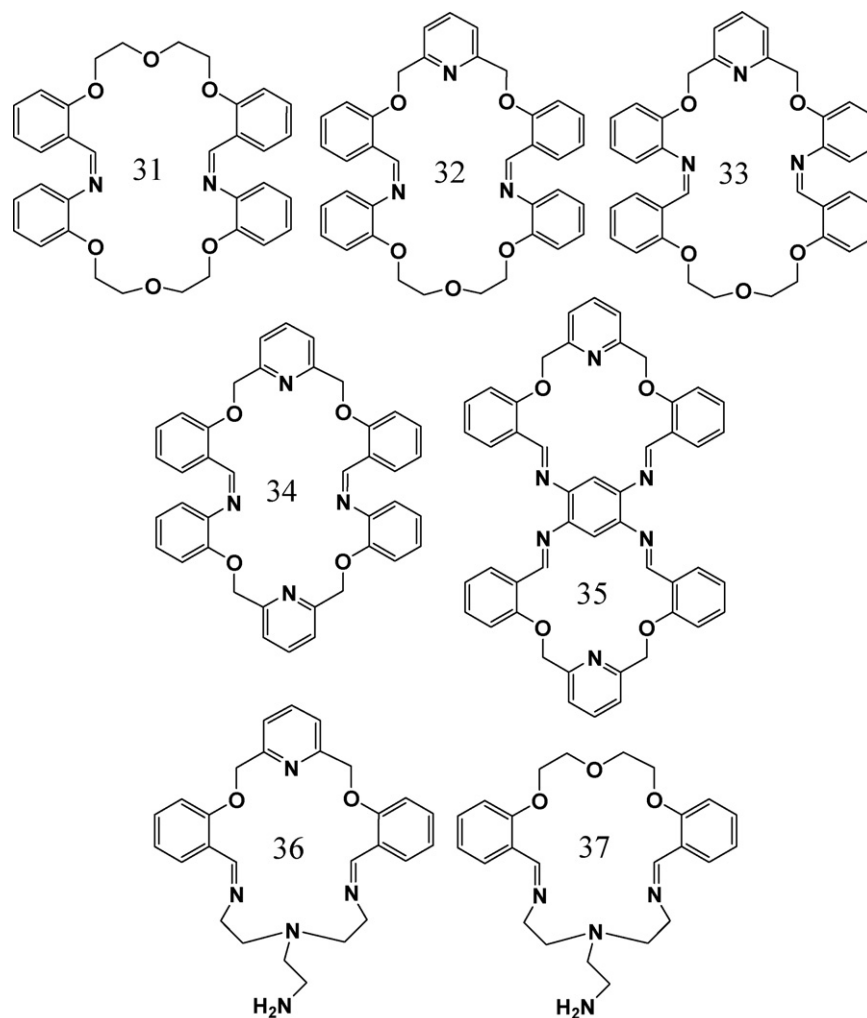


Fig. 23. Schematic representation of the ATP hydrolysis by the mononuclear $\text{Zn}^{2+}/\text{25}$ complex in water at pH 4. Distribution diagram for the system $\text{Zn}^{2+}/\text{25}/\text{ATP}$ in 2:1:1 molar ratio (—, left y-axis) and experimental pseudo-first-order rate constants (●, right y-axis) for ATP hydrolysis at 298.1 K ($I = 0.1 \text{ M}$, $[\text{ZnL}] = [\text{Zn}^{2+}] = 1.65 \times 10^{-2} \text{ M}$) [65].



Scheme 14.

38, as shown by the X-ray diffraction, no emission was observed, see Fig. 24, due to photoelectron transfer that take place from the non-protonated nitrogen [67]. Similar results were observed for macrocycles **39** and **42**.

Another example of the appearance of fluorescence upon reduction of the imine C=N bond to a C–NH amine bond was observed for compounds **37** and **40**. While compound **37** is not emissive in solution, compound **40** reveals fluorescence properties in water, see Fig. 25.

The binding properties of macrocyclic **40** towards Cu^{2+} , Zn^{2+} , Cd^{2+} and Pb^{2+} were studied by potentiometry, absorption and fluorescence spectroscopies. The behaviour of this system is quite similar to the one reported for the polyamine-based receptors [67]. All the Cu^{2+} complexes species exhibit a strong CHEQ effect attributed to an energy transfer quenching of the π^* emissive state though low-lying metal-centered states [68].

On the other hand, Zn^{2+} and Cd^{2+} complexes are emissive species leading to a CHEF effect. Fig. 25A compares the titration curves of **40** in the absence and in the presence of three different cations in order to evaluate the chemosensor ability of the ligand towards Cu^{2+} , Zn^{2+} and Cd^{2+} .

The titration curves of these metals exhibit different fluorescence responses for $\text{pH} \geq 4$, and below this value only protonated forms of ligand **40** are present in solution. The fluorescence of ligand **40** in the presence of alkaline and alkaline-earth metals and some

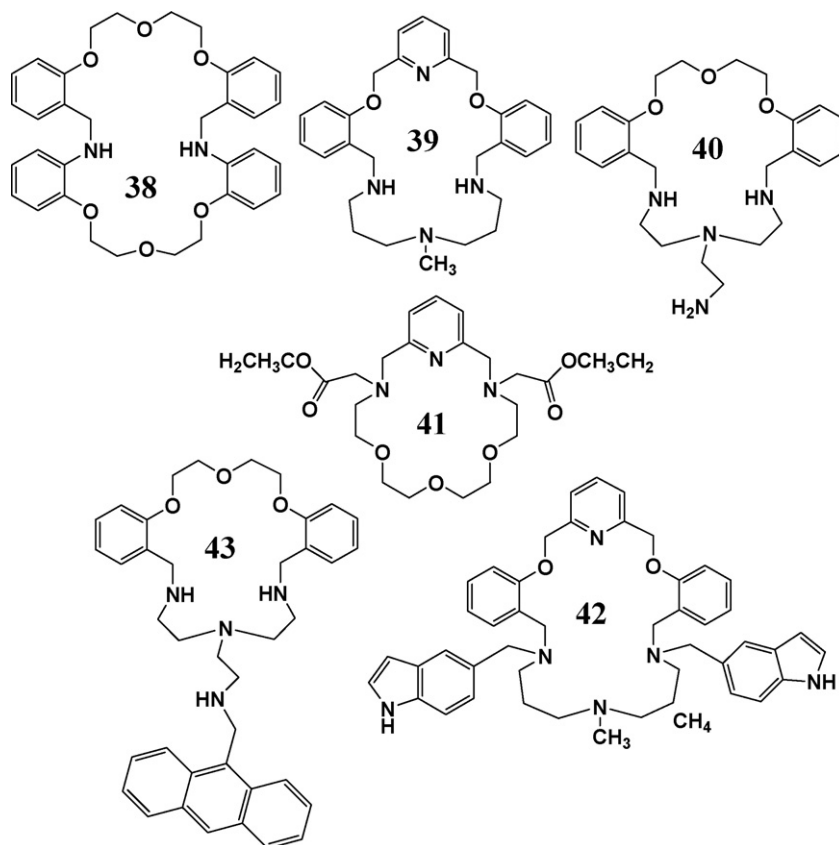
transition metal ions such as Co^{2+} , Ni^{2+} and Hg^{2+} were also studied. Only small changes on the fluorescence intensity were observed, except for Co^{2+} and Hg^{2+} for which a CHEQ effect similar to Cu^{2+} was achieved. The fluorescence response of this system at pH 7.45 to these metal ions is summarized in Fig. 25B.

The enhancement of fluorescence in the presence of Zn^{2+} is almost independence of a huge excess of Li^+ , K^+ , Mg^{2+} and Ca^{2+} (up to 1:100). The increase observed in the fluorescence emission upon Zn^{2+} complexation can be understood from the type of coordination of this metal. Fig. 26 shows the X-ray structure of the complexes $[\text{40Zn}]^{2+}$, which shows that the metal ion is coordinated by all nitrogen atoms present in the ligand preventing the PET quenching effect.

In order to separate the binding function to the signaling function an anthracene pendant-arm was introduced in ligand **40**, see ligand **43** [69].

This strategy allows one to obtain a chemosensor exhibiting a more intense and red-shifted fluorescence emission. The fluorescence response of **43** is similar to the parent ligand **40**. In this case the interaction with Al^{3+} and Cr^{3+} in methanol or water/methanol solutions was studied and the CHEF effect, leading an increase of 1.80-fold for Al^{3+} and 2.0-fold for Cr^{3+} was observed, see Fig. 27.

Macrocyclic ligand **41** possessing two carboxylic acids as pendant-arms was studied in acetonitrile, water and mixtures of water/acetonitrile solutions [70]. The ligand is non-emissive in



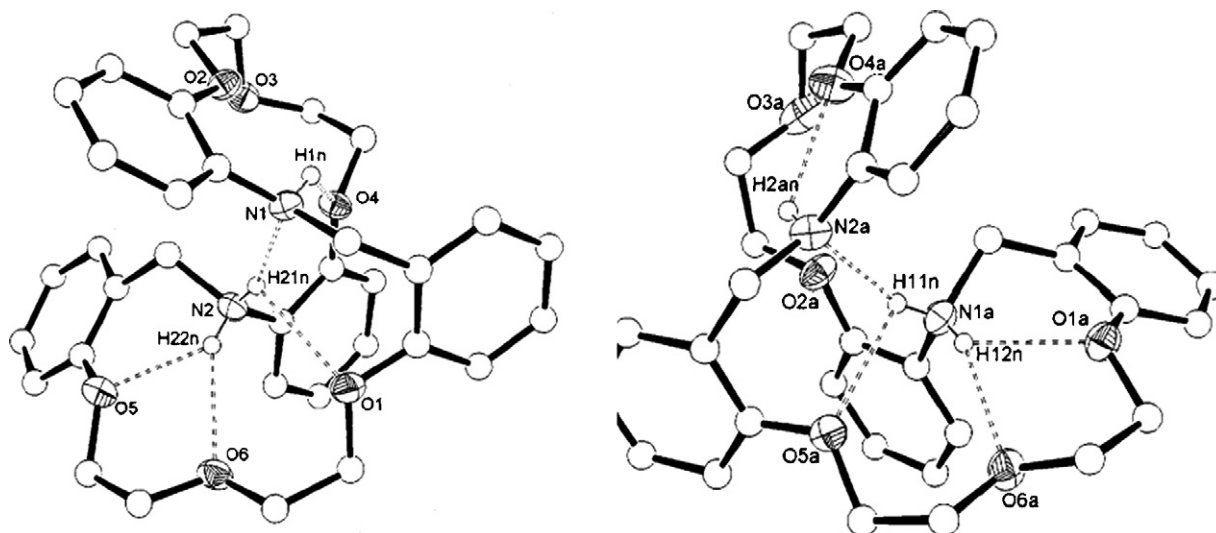
Scheme 15.

solution as well in the presence of several metal ions such as alkaline, alkaline-earth and transition metals [70]. However, similarly to that observed with polyamine 29, the characteristic visible emission bands from complexes of Eu^{3+} and Tb^{3+} in water at 618 and 586 nm, respectively were observed, upon excitation at *ca.* 270 nm.

In conclusion, while the introduction of the oxygen atoms in these families of compounds extend the number of metal ions capable of binding the receptor, no significant improvements were obtained in comparison with the polyamine systems. Modifying the

N_xO_y donor-sets into more flexible acyclic structures, several Schiff-base or reduced-amine bis-chromophoric ligands were synthesized [71] (Scheme 16).

In the case of ligand **44**, and similarly to other Schiff-base macrocycles, no fluorescence emission was detected for the free ligand or after complexation with metal ions. In contrast, compound **45** in acetonitrile-water solution shows fluorescence emission band centered at 365 nm, attributed to the 15-benzocrown-5 moiety [71a]. This emission is quenched by Cu^{2+} , Pb^{2+} and Al^{3+} complexation as

Fig. 24. Molecules 1 and 2 of the protonated macrocycle **38** in the asymmetric unit of $[(\mathbf{38})\text{H}](\text{ClO}_4) \cdot \text{CHCl}_3$ [67a].

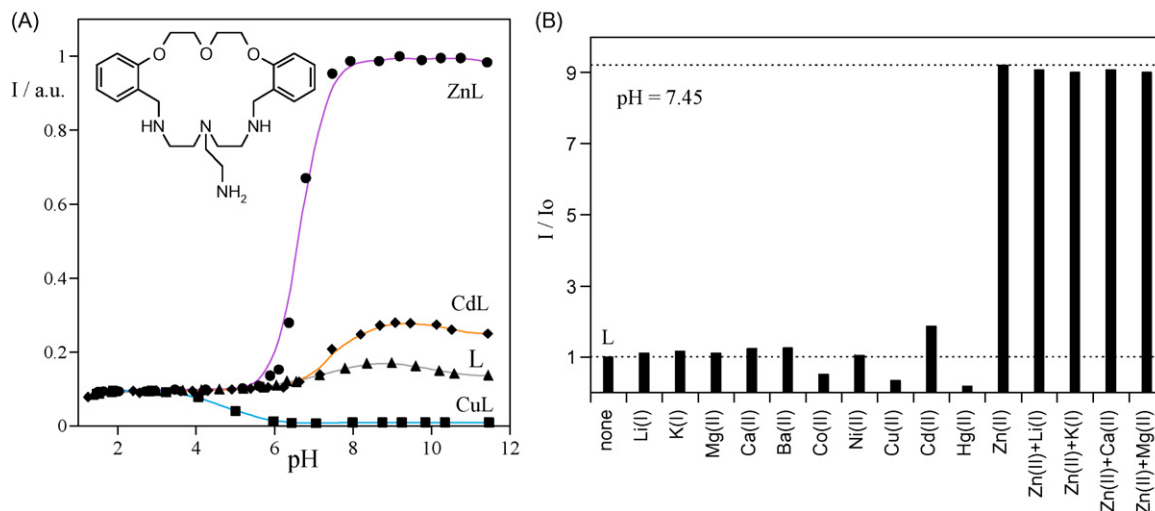


Fig. 25. (A) Fluorescence emission titration curves of **40** (▲) in the presence of equimolecular amounts of Cu^{2+} (■), Cd^{2+} (◆) and Zn^{2+} (●). ($\lambda_{\text{exc}} = 275 \text{ nm}$, $\lambda_{\text{em}} = 303 \text{ nm}$, $[\mathbf{40}] = 4.95 \times 10^{-5} \text{ M}$, $[\text{NaCl}] = 0.15 \text{ M}$), and (B) relative fluorescence intensity at 303 nm of **40** ($4.70 \times 10^{-5} \text{ M}$) in the absence of metal ions at pH 7.45. Presence of an excess amount (up to 1:100) of Li^+ , K^+ , Ca^{2+} and Mg^{2+} are represented in the last four columns, respectively [67j].

was previously observed in the parent ligand, 15-benzo crown-5, with alkaline ions [72].

Interesting color changes in the absorption spectra from yellow to blue-violet (absorbance at 590 nm) were observed upon Cu^{2+} complexation with **44** or **45**. Under the same conditions other transition metal ions studied (Zn^{2+} , Ni^{2+} , Co^{2+} , Cd^{2+} , Pb^{2+} and Al^{3+}) gave non-significant effects, and thus **44** or **45**, could be used as a colorimetric chemosensor to determine the presence of Cu^{2+} in acetonitrile solution. For **44**, the absorbance increase was linear up to $1.05 \times 10^{-4} \text{ M}$, for **45**, the linearity in the absorption was up to $5.30 \times 10^{-5} \text{ M}$.

The pyrene-derivatives **46** and **47** were synthesized in order to take profit from the well-known pyrene excimer emission [71b]. The fact that the most intense excimer emission takes place in compound **47** most probably arises because its structure is more flexible than in compound **46**.

The fluorescence emission titration curve of **47** (Fig. 28A), shows the typical profile of chemosensors bearing both, aliphatic and aromatic nitrogen atoms in the receptor unit, see above. According

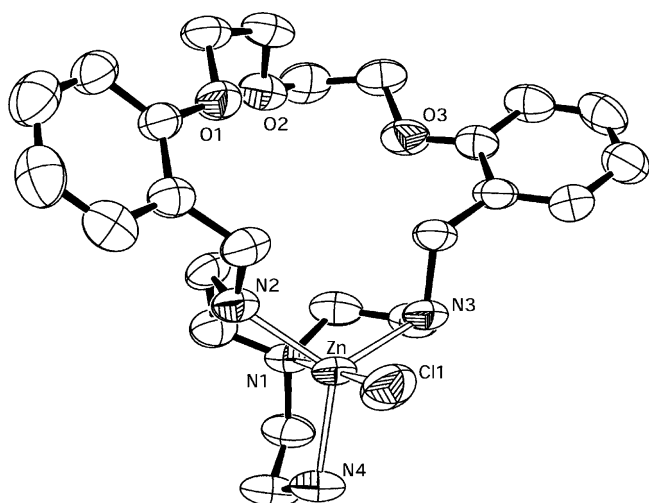


Fig. 26. X-ray crystal structure of $[\text{Zn}(\mathbf{40})\text{Cl}](\text{ClO}_4) \cdot \text{H}_2\text{O}$ showing 50% probability thermal ellipsoids [67j].

to literature data obtained with similar receptor units, compound **46** makes stronger complexes with Cu^{2+} and Zn^{2+} in comparison with **47**. This is in agreement with the results reported in Fig. 28B and C, where complexation with these metals disrupts the excimer in compound **46** while it is a minor effect in compound **47**. On other hand, compound **47** is better sensor for organic dyes, such as the barbituric acids. In this case, formation of the excimer is prevented most probably by inclusion of the dye into the receptor cavity, resulting in a decrease of the excimer accompanied by an increase of the monomer emission.

In order to obtain efficient emissive metal complexes keeping in mind potential applications as new OLEDs, the acyclic ligands **48–50** were studied in the presence of Zn^{2+} and Cd^{2+} in collaboration with Bermejo [71c–d]. The most relevant results were obtained with compound **50** in solid state in the presence of carboxylate dyes, see below. Both free ligands exhibit weak fluorescence emission in

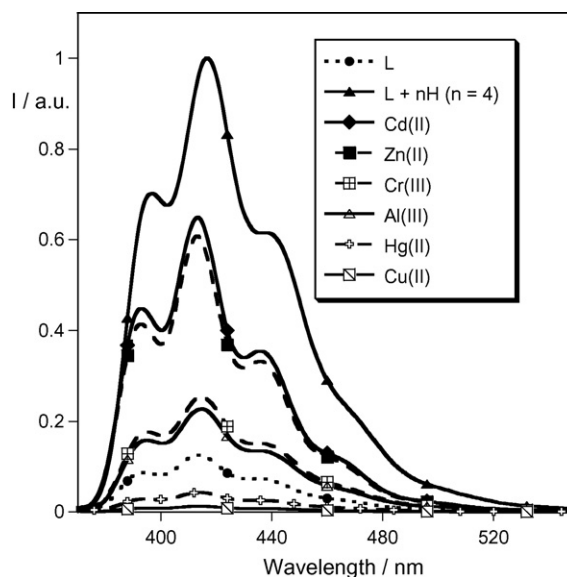


Fig. 27. Fluorescence emission spectra of methanol solutions of **43** in the presence of one equivalent of $\text{Zn}(\text{NO}_3)_2$, $\text{Cd}(\text{NO}_3)_2$, $\text{Cr}(\text{NO}_3)_3$, AlCl_3 , $\text{Hg}(\text{CF}_3\text{SO}_3)_2$ and $\text{Cu}(\text{CF}_3\text{SO}_3)_2$. ($[\mathbf{43}] = 1.25 \times 10^{-5} \text{ M}$, $\lambda_{\text{exc}} = 367 \text{ nm}$) [69].

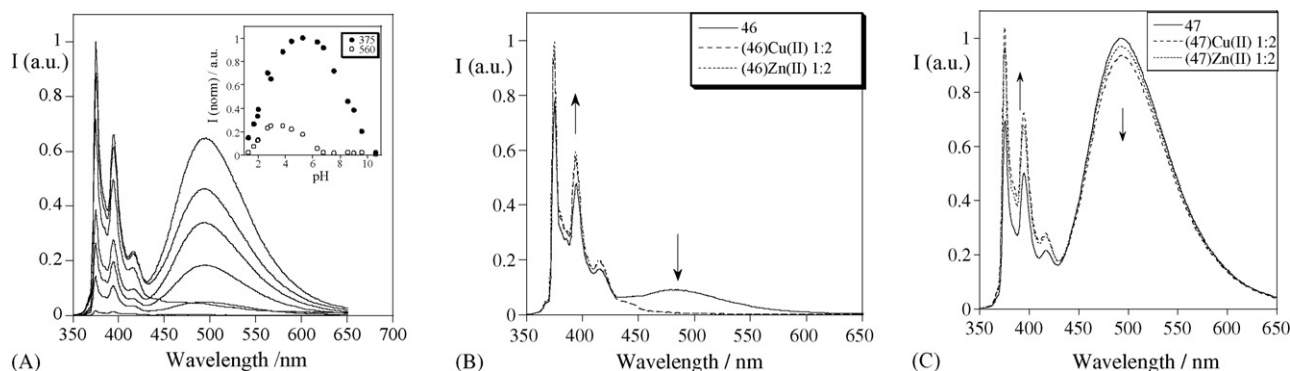
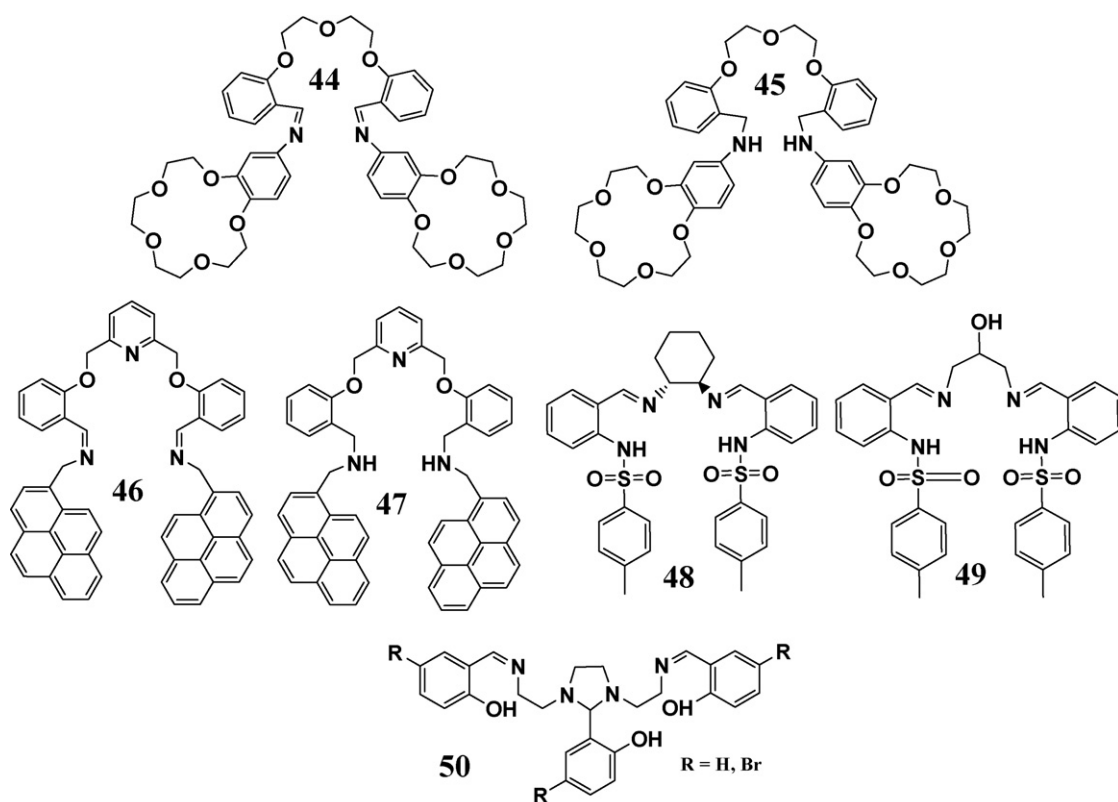


Fig. 28. (A) Emission spectra of ligand **47** in 95.5%water–0.5% acetonitrile solution as function of pH; pH 1.32, 1.69, 2.04, 3.84, 5.3, 7.6 and 11.10), (B) emission spectra of the ligand **46** in CH_2Cl_2 (black line), and (C) emission spectra of compound **47** in 95.5%water–0.5% acetonitrile solution (black line) (right) and **47** in the presence of two equivalents of Cu^{2+} and Zn^{2+} ($\lambda_{\text{exc}} = 343 \text{ nm}$, 25°C , $[\text{46,47}] = 6.00 \times 10^{-6} \text{ M}$) at pH 5.15 [71b].



Scheme 16.

absolute ethanol solution upon excitation at 315 (H) nm and 404 (Br) nm, respectively. Upon Zn^{2+} complexation, a large increase in the fluorescence emission was observed with maxima at 455 and 450 nm, and quantum yields of 0.11 and 0.09, respectively.

The synthesis of multinuclear zinc(II) complexes using carboxylate donors such as ortho-phthalate, 4-formylbenzenecarboxylate, malonate, succinate or terephthalate were reported with ligand **50** [71e]. According to the X-ray structure bi and tetranuclear compounds bridged by carboxylated donors were obtained see Fig. 29. All the (yellow) solids are emissive and exhibit moderate to strong fluorescence quantum yield (0.19–0.54). The color of the emitted light can be modulated by complexation with different carboxylated compounds from λ_{max} 450 to 590 nm, see Fig. 29. This effect could be explored as an attractive alternative to the usual inorganic hybrid materials used as the active layer in the light-emitting diode devices (LEDs) and lasers [73].

7. Emissive polythia-aza-based receptors

According to the Pearson rules [66], receptor units containing soft donors such as sulfur atoms, with stronger nucleophilicity than oxygen, permit one to recognize soft metals with marked thiophilicity, such as Cd^{2+} , Hg^{2+} , Pd^{2+} and Ag^+ , better than with polyamine or polyoxa-aza systems. On this basis, a family of these compounds (Scheme 17) was synthesized and studied in collaboration with Casabó and Escriche.

The absorption and fluorescence emission in freshly dry dichloromethane solution of **51–53**, shows the expected trend for a receptor containing aliphatic-aromatic amines. The aliphatic amine is protonated upon addition of the first proton equivalent, resulting in a red-shift in the absorption spectrum and an increase of the fluorescence emission intensity. Addition of successive equivalents of protons shows an increasing in the absorption spectrum,

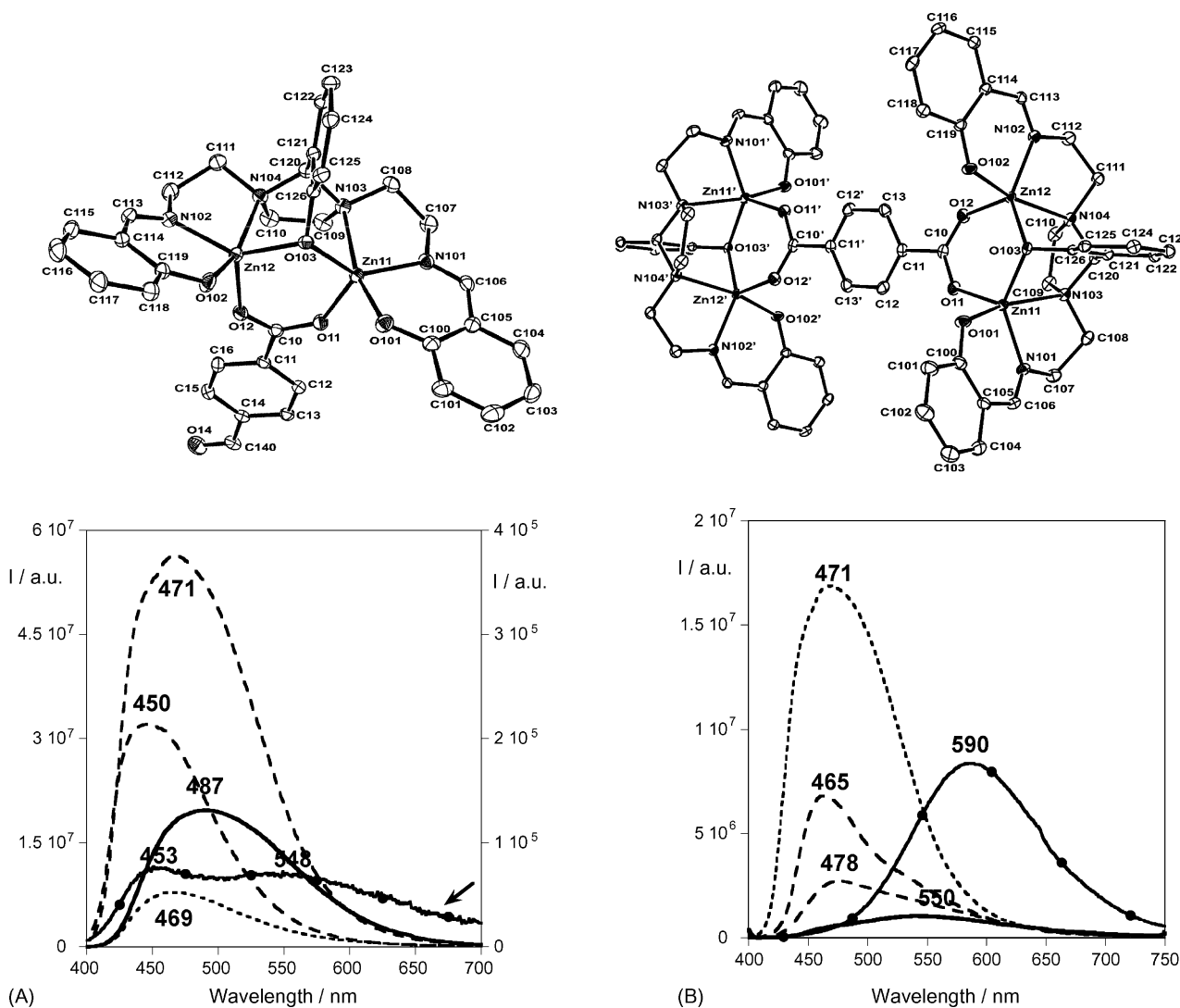
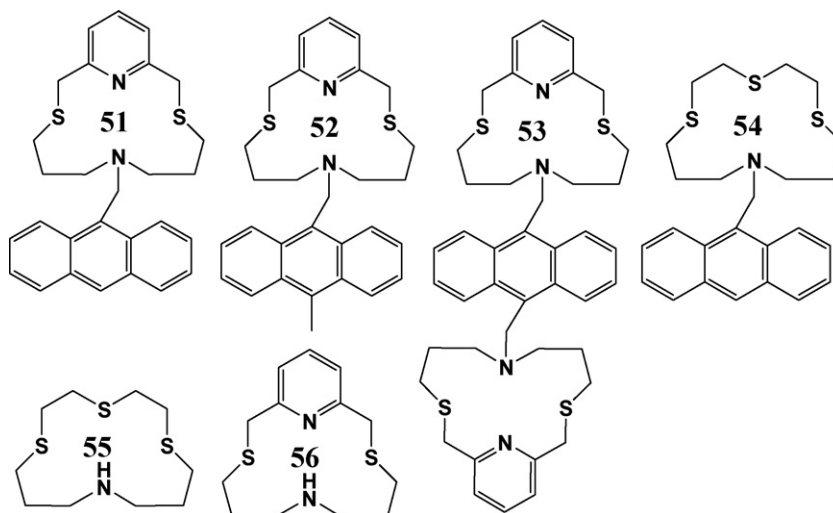
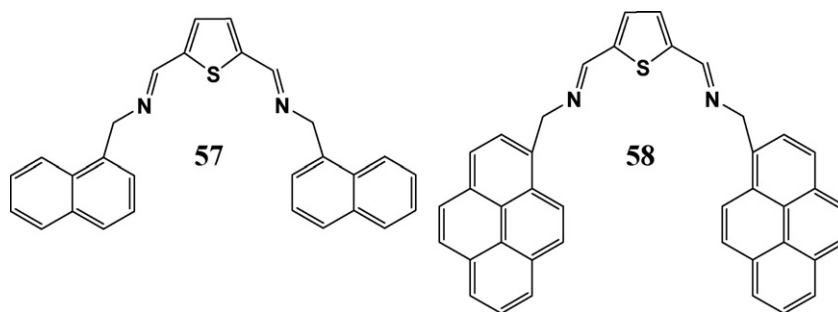


Fig. 29. X-ray molecular structures of [Zn₂50(p-OOC-C₆H₄CHO)]·2.5DMSO·2H₂O and [(Zn₂50)₂(p-OOC-C₆H₅-COO)]·2.5H₂O·MeOH·6EtOH. Emission spectra in solid state at 298 K for: (A) Zn²⁺ complexes of **50** (R=H), $\lambda_{\text{exc}} = 370$ nm; (B) Zn²⁺ complexes of **50** (R=Br), $\lambda_{\text{exc}} = 380$ nm. A tuning in the light color emitted is observed as function of the carboxylate donor present in the complex [71e].



Scheme 17.



Scheme 18.

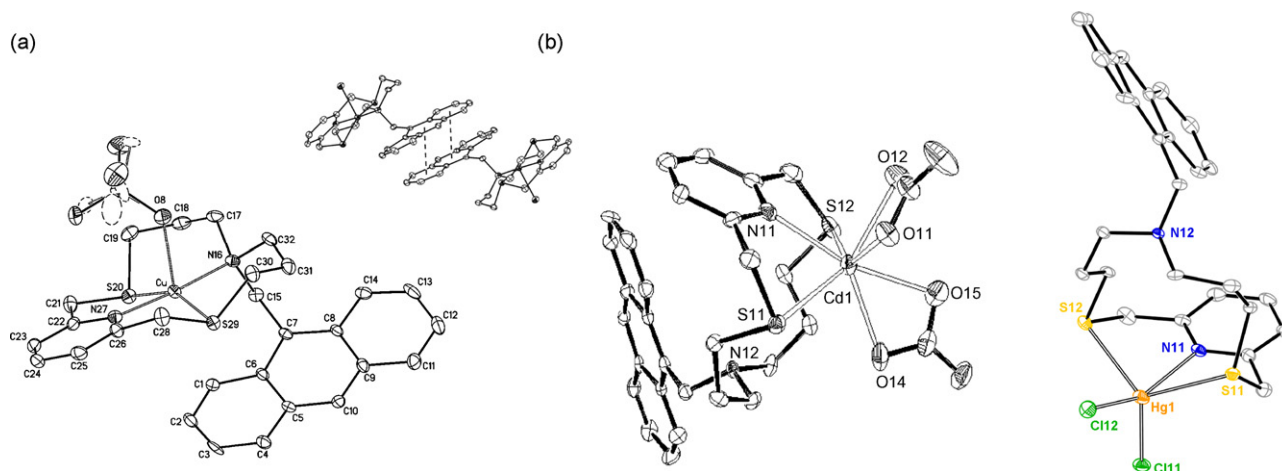


Fig. 30. X-ray structures of complexes (A) $[\text{Cu}(\text{ClO}_4)(\mathbf{51})]^+$ ion, (B) $[\text{Cd}(\text{NO}_3)_2(\mathbf{51})]$, and (C) $[\text{HgCl}_2(\mathbf{51})] \cdot 1/2\text{CH}_2\text{Cl}_2$ (ellipsoids at 40% (Cu^{2+} and Cd^{2+}) and 30% (Hg^{2+}) probability level). Hydrogen atoms and dichloromethane molecules are omitted for clarity. In the copper(II) complex a perspective view of dimers of $[\text{Cu}(\text{ClO}_4)(\mathbf{51})]$ with the $\pi \cdots \pi$ interactions is shown [74a,75,76].

and a decrease in the fluorescence emission intensity, both effects compatible with pyridinium formation [74,75] (Scheme 17).

Several emissive mononuclear complexes have been obtained with ligands **51** and **52**, while dinuclear species were obtained for

53. Fig. 30 shows the X-ray structures of complexes $\text{Cu}(\mathbf{51})$, $\text{Cd}(\mathbf{51})$ and $\text{Hg}(\mathbf{51})$. As can be observed, copper is coordinated by all the N_2S_2 donor atoms present in the ligand, while $\text{Cd}(\text{II})$ and $\text{Hg}(\text{II})$ are not coordinated to the tertiary amine nitrogen. For complexes

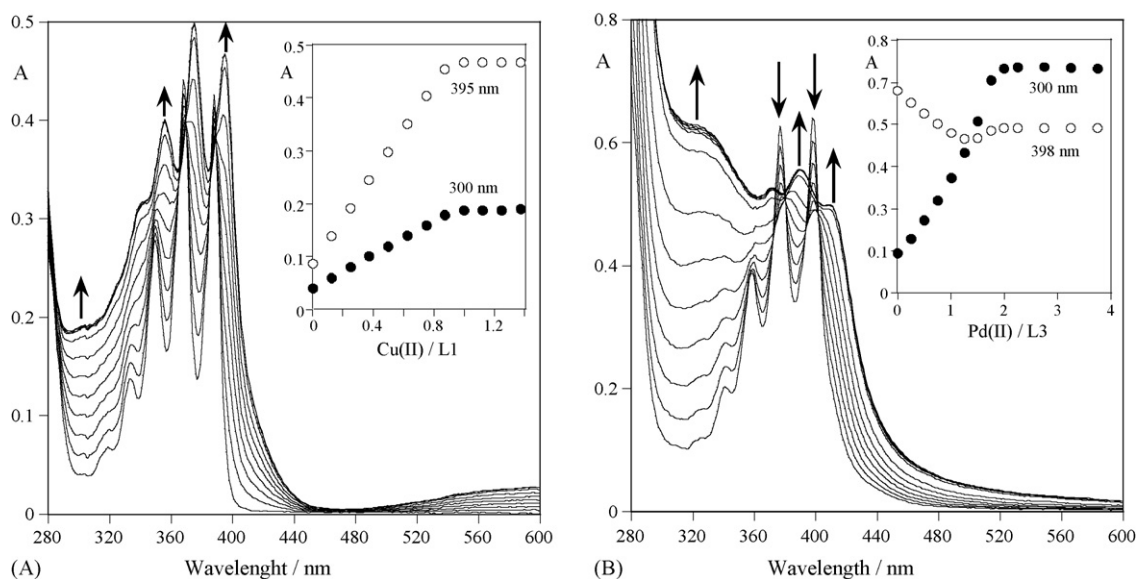


Fig. 31. (A) Absorption spectra of a dichloromethane solution of **51** as a function of added $\text{Cu}(\text{CF}_3\text{SO}_3)_2$. The inset shows the absorbances at 300 and 395 nm. (B) Absorption spectra of a dichloromethane solution of **53** as a function of added $\text{Pd}(\text{BF}_4)_2$. The inset shows the absorbances at 300 and 398 nm. ($[\mathbf{51}] = 4.73 \times 10^{-5} \text{ M}$, $[\mathbf{53}] = 5.55 \times 10^{-5} \text{ M}$) [74a,77].

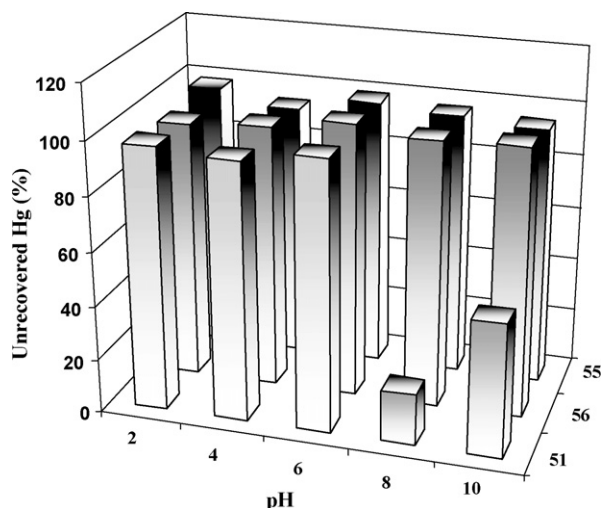


Fig. 32. Unrecovered Hg^{2+} remaining in aqueous phase after treatment with dichloromethane solutions of **51**, **55** and **56**, at different pH values [76].

with **51** and **52**, a red-shift in the absorption spectra compatible with 1:1 complexation, while 1:2 (L:M) with **53** was observed (see Fig. 31). Concerning the fluorescence emission, Cu^{2+} and Hg^{2+} lead to a CHEQ while Cd^{2+} to CHEF effects. In this last case, protonation of the aliphatic amine is expected, a result that is compatible with the X-ray structure. A CHEF effect was observed for Zn^{2+} and Ag^{+} complexes, and Pd^{2+} leads to a CHEQ effect with the same ligands. Identical behaviour was observed with the anthracene derivative ligand **54** [76].

In order to explore the analytical applications of this family of ligands, extraction experiments were performed to assess the capability of ligands **51**, **55** and **56** to remove mercury from aqueous solution. As can be seen in Fig. 32, only ligand **51** was able to effectively remove Hg^{2+} from aqueous solution, explained by the more hydrophobic characteristic of ligand **51** when compared with ligands **55** and **56**. As expected the extraction capability of **51** is less efficient at low pH values due to the proton competition for the receptor binding.

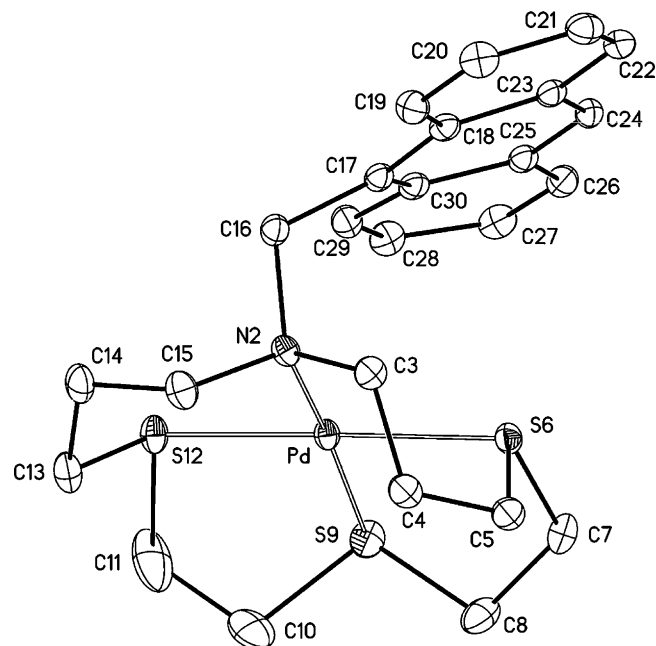


Fig. 34. X-ray structure of the $[\text{Pd}(\mathbf{54})]^{2+}$ cation with the atom-numbering scheme adopted [77].

Addition of one equivalent of proton to ligand **54** followed by titration with Pd^{2+} is shown in Fig. 33 [77]. The fluorescence emission and excitation spectra show the characteristic bands of the anthracene systems. An “Off-on-off” behaviour of the fluorescence was observed as follows. The dichloromethane solution of free ligand **54** is weakly emissive (Off). When an equivalent of acid is added to a ligand a CHEF effect is observed (On). Addition of one equivalent of Pd^{2+} causes strong quenching of the fluorescence (Off) see Fig. 33.

The crystal structure of the Pd^{2+} confirms the mononuclearity observed in solution for this complex, and consists of discrete $[\text{Pd}(\mathbf{55})]^{2+}$ cations and tetrafluoroborate anions (see Fig. 34).

Introduction of the sulfur donor atom into the fluorescence chemosensor skeleton, was also achieved in compounds **57** and **58**,

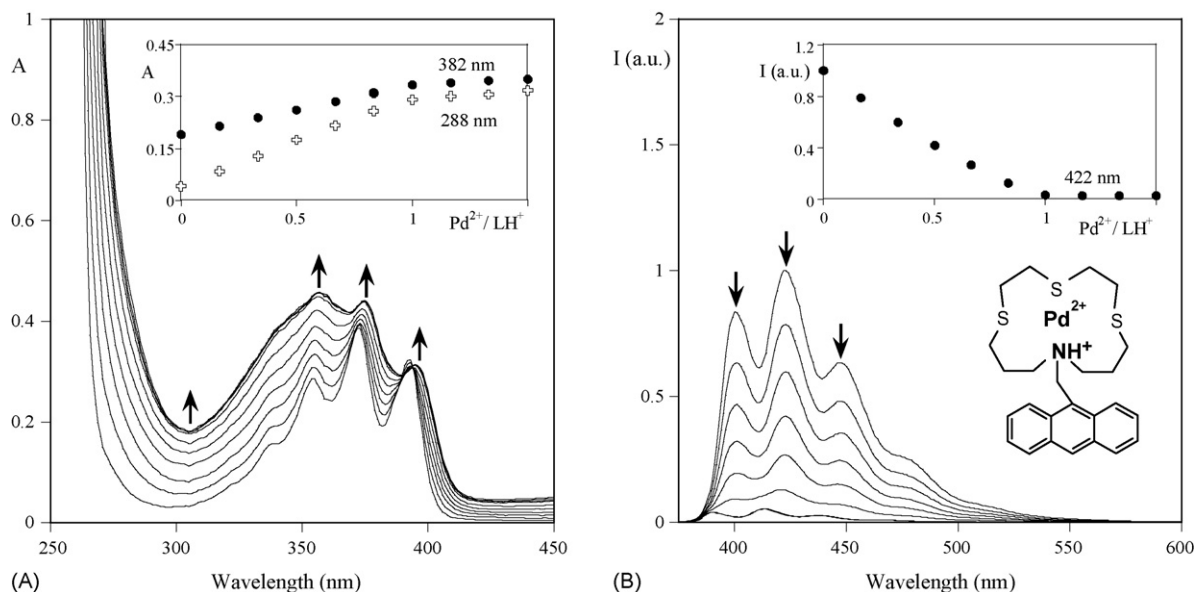


Fig. 33. Absorption spectra (A) and emission spectra (B) of $\mathbf{54H}^{+}$ as a function of increasing amounts of $\text{Pd}(\text{BF}_4)_2$. The inset shows the absorbances at 288 and 382 nm (A) and the normalized fluorescence intensity at 422 nm. (B) ($[\mathbf{54}] = [\mathbf{54H}^{+}] = 5.14 \times 10^{-5} \text{ M}$, $T = 298 \text{ K}$, $\lambda_{\text{exc}} = 368 \text{ nm}$) [77].

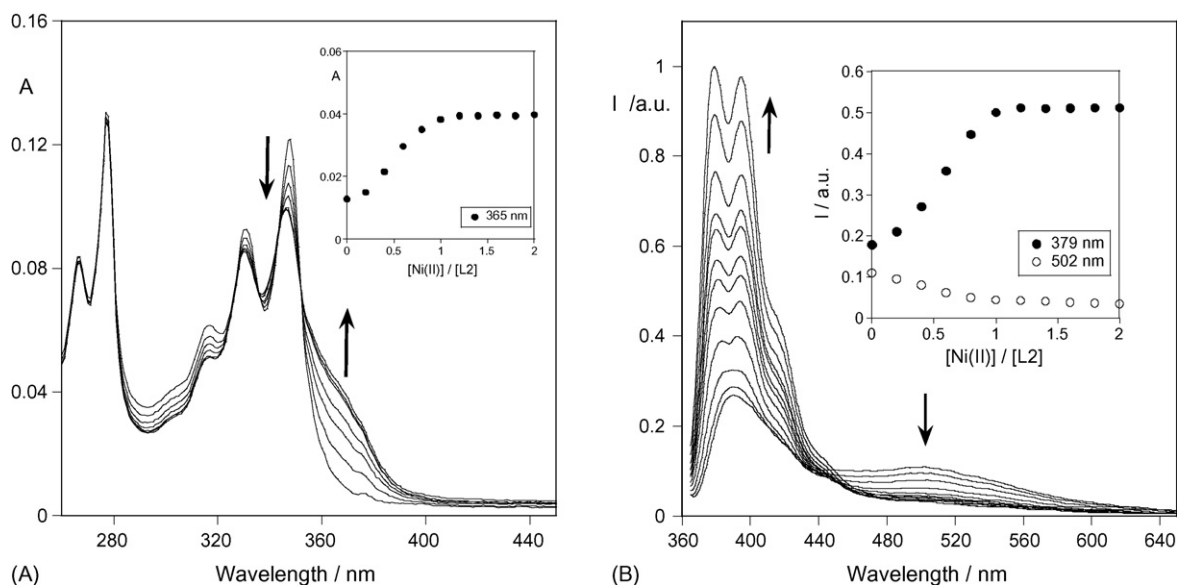


Fig. 35. Absorption (A) and fluorescence (B) spectra of **58** in the presence of Ni(II) (concentration range 0–2 equivalents), in dichloromethane solution ($[\mathbf{58}] = 1 \times 10^{-6}$ M, $\lambda_{\text{exc}} = 350$ nm). Inset shows (A) absorption at 365 nm and (B) intensity of emission as function of $[\text{Ni}^{2+}]/[\mathbf{58}]$ at $\lambda_{\text{em}} 379$ nm (monomer) and 502 nm (excimer) [78].

by the condensation of an aromatic species such as the thiophene unit [78] (Scheme 18).

Both ligands were explored as metal chemosensors in solution and in the solid state [78]. Solid metal complexes were obtained by direct reaction between ligands **57** and **58** and the $\text{Ni}(\text{ClO}_4)_2 \cdot 6\text{H}_2\text{O}$ and $\text{Pd}(\text{BF}_4)_2 \cdot 4(\text{CH}_3\text{CN})$ metal salts. In all cases,

mononuclear complexes were isolated and characterized. Concerning the free ligands, absorption and emission studies were performed in dichloromethane solution. Ligand **57** is not emissive, while ligand **58** shows the characteristic pyrene monomer emission ($\lambda_{\text{exc}} = 340$ nm) centered at 400 nm and a low intensity excimer band, centered at 525 nm (Fig. 35B). In the solid state, the monomer

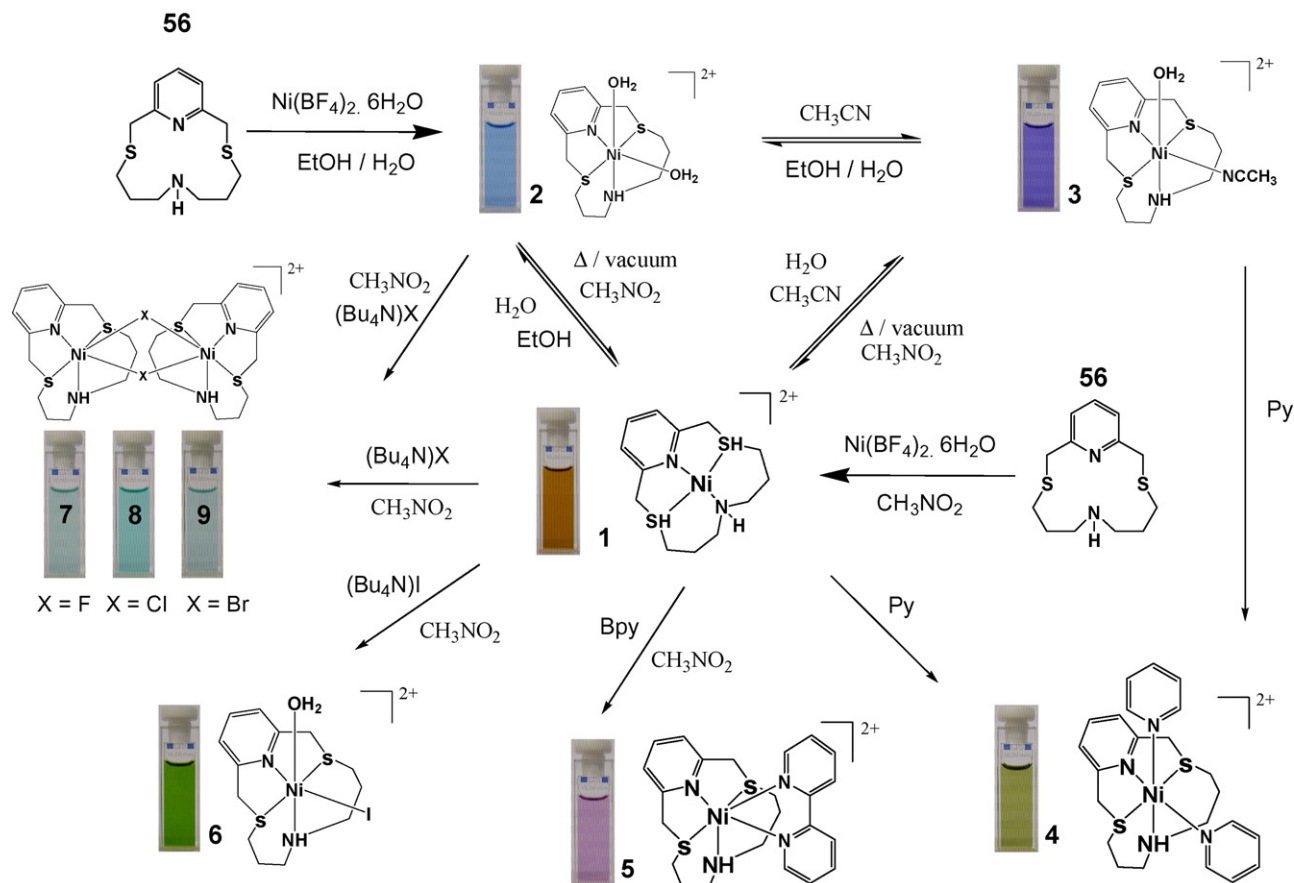


Fig. 36. Complex Ni^{2+} (**56**) in the presence of CH_3CN , H_2O , pyridine, 2,2'-bipyridine, fluoride, chloride, bromide and iodide in nitromethane [79].

band disappears and the excimer emission increases in intensity and is red-shifted (580 nm).

In solution as well as in solid state, the mononuclear complexes of Ni^{2+} and Pd^{2+} with **57** are not emissive, while with **58** the excimer emission disappears with concomitant increase of the monomer emission in both cases.

MALDI-TOF-MS studies were performed with ligand **57** and **58**. A solid layer of ligand was deposited on the MALDI-TOF-MS plate followed by superposition of a second solid layer of the mentioned metals without matrix. An *in situ* MALDI-TOF reaction on the system takes place upon laser irradiation, and formation of the metal complexes was observed with compound **58**, while no complexation was achieved with compound **57**.

In Fig. 35 is shown the absorption and fluorescence titration with ligand **58** in the presence of increasing amounts of Ni^{2+} . As was reported for ligand **46** reported below, complexation with metals disrupts the interaction between both pyrene rings, and as a consequence the excimer emission disappears.

8. Chromogenic complexes containing sulfur donor receptors for recognition effects

The use of color changes upon complexation of analytes is probably the simplest way of carrying out a chemical analysis because color is immediately perceived by the naked eye. In spite of the use of many other much more sophisticated and precise alterna-

tives, in some cases, the change of color is still a useful tool. A straightforward way to obtain color changes is the use of complexes coordinatively unsaturated or containing labile ligands which can easily be replaced. Ligand **56** fulfills these requirements (see Fig. 36 [79,74b]).

Reaction of compound **56** with one equivalent of Ni^{2+} perchlorate or tetrafluoroborate in ethanol, gives a blue solution from which it is possible to extract crystals with the formula $\text{Ni}(\textbf{56})(\text{H}_2\text{O})_2(\text{X})_2$ ($\text{X} = \text{ClO}_4, \text{BF}_4$). X-ray diffraction analysis of the perchlorate derivative shows the Ni^{2+} ion in a distorted octahedral environment (see compound **2** in Fig. 36). Addition of acetonitrile to the ethanol solution gave a purple compound. The X-ray structure of the new crystals precipitated from the acetonitrile solutions shows the presence of this solvent in the coordination sphere (See compound **3** in Fig. 36).

When the reaction between **56** and Ni^{2+} tetrafluoroborate was carried out in anhydrous nitromethane or dichloromethane instead of ethanol, the color of the resulting solution was red and a square planar complex was obtained (see compound **1** in Fig. 36).

Addition of coordinating solvent molecules, such as acetonitrile or absolute ethanol (not dried), to nitromethane solutions of **1** changes the geometry of the nickel ion from square-planar to octahedral, leading, respectively to compounds **3** and **2**. This process is reversible and recovery of compound **1** can be achieved by heating and removing the solvents under vacuum.

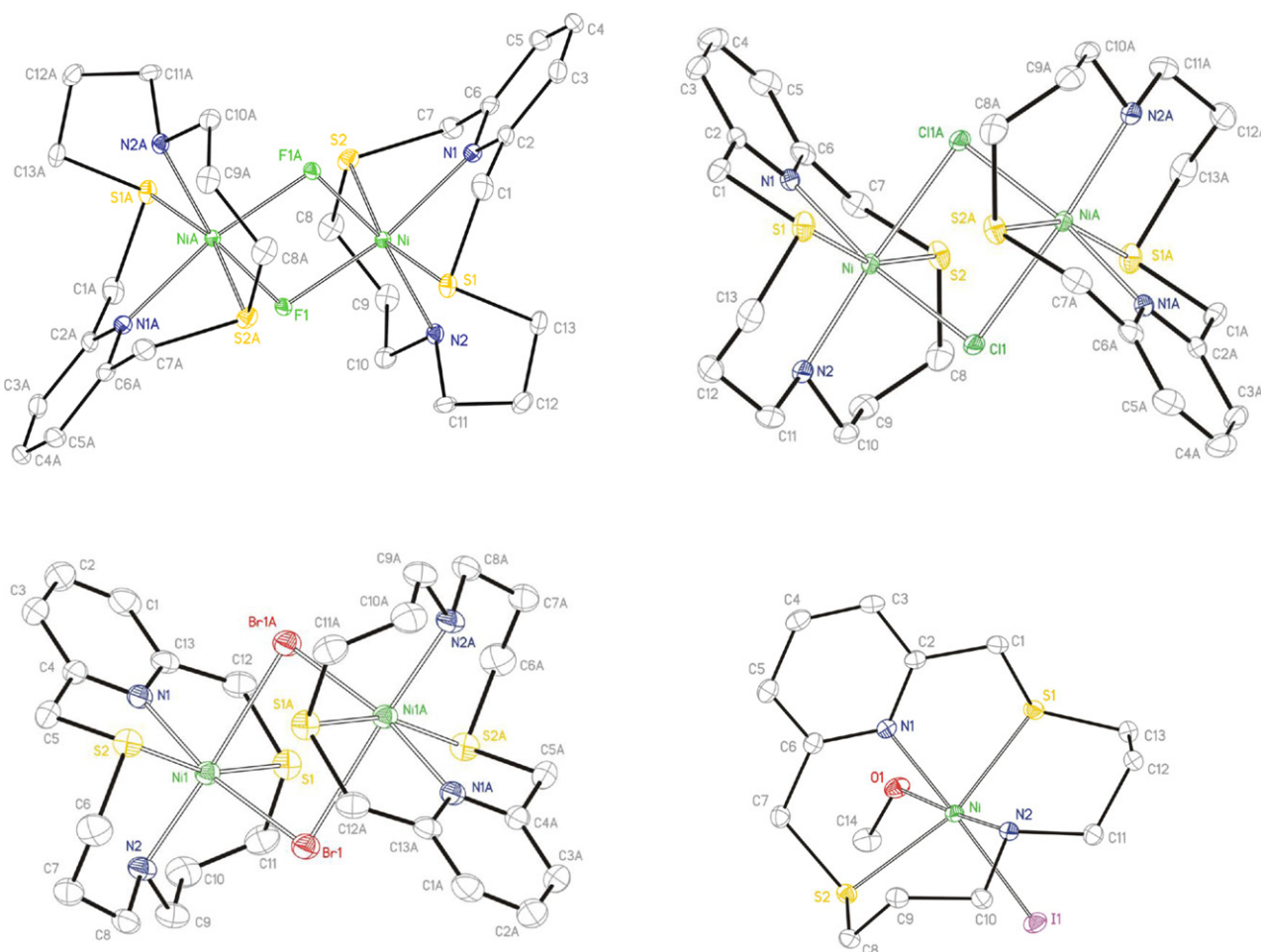
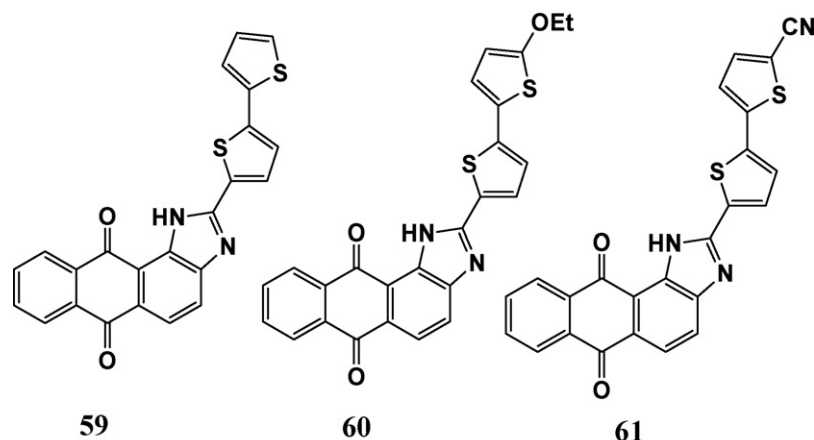


Fig. 37. Structure of complexes $[\{\text{Ni}(\textbf{56})\}_2(\mu\text{-F})_2]^{2+}$, $[\{\text{Ni}(\textbf{56})\}_2(\mu\text{-Cl})_2]^{2+}$, $[\{\text{Ni}(\textbf{56})\}_2(\mu\text{-Br})_2]^{2+}$ and $[\text{Ni}(\text{CH}_3\text{OH})(\textbf{56})]^+$ with the atom-numbering scheme adopted. Ellipsoids are shown at the 40% probability level. Non-coordinated counterions and hydrogen atoms were omitted for clarity [79,80].



Scheme 19.

The red color of dichloromethane solutions of **1** turns from red to pink or yellow-green, by adding of 2,2'-bipyridine and pyridine, respectively (see compounds **5** and **4** in Fig. 36). Both processes are irreversible.

The addition of iodide to **1**, leads to dark green solution of a mononuclear octahedral complex, see compound **6**. Finally, cyan solutions were obtained by adding fluoride, chloride or bromide (see compounds **7**, **8** and **9** in Fig. 36) giving dinuclear complexes in

which two halide ions bridge two compound **1** moieties. This last behaviour can be explored as a probe for detecting iodide ions in solution.

The X-ray structures of the fluoro, chloro and bromo derivatives are shown in Fig. 37. The larger the halide ion the more asymmetric the $\text{Ni}(\mu\text{-X})_2\text{Ni}$ core, which in the limit leads to the formation of monomeric species with iodide ions. The length of these bridges affects notably the magnetic properties of these Ni^{2+} (**54**)

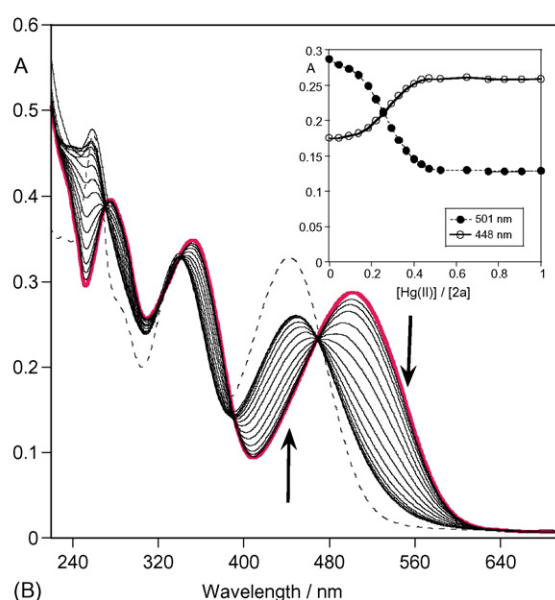
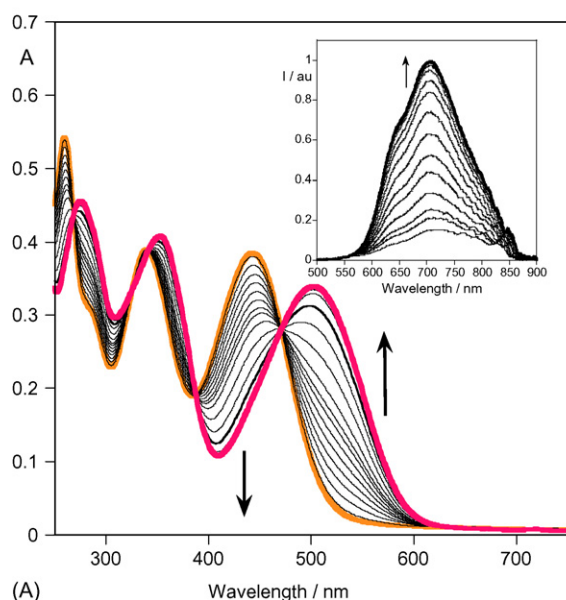
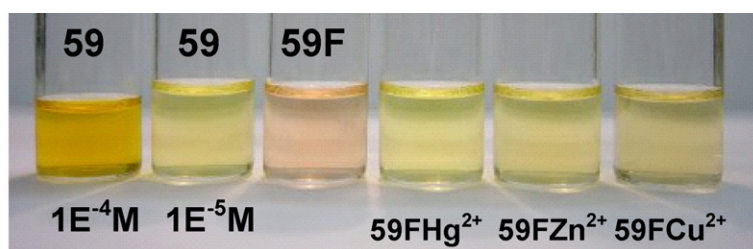


Fig. 38. (A) Changes in UV-vis and fluorescence spectra of compound **59** in acetonitrile with addition of a solution of $[(\text{Bu})_4\text{N}]\text{F}$ acetonitrile solution. (B) UV-vis spectra of $\text{F}(\mathbf{59})$ species with increasing amount of $\text{Hg}(\text{CF}_3\text{SO}_3)_2$ added. Dotted line spectra: free ligand. Colorimetric effect in compound **59** after the interaction with fluoride, fluoride and Hg^{2+} , fluoride and Zn^{2+} and fluoride and Cu^{2+} [81].

complexes [80]. Intramolecular interactions were observed in the three-dinuclear complexes, being antiferromagnetic in the fluoro derivative and ferromagnetic in both, the chloro and bromo compounds. The iodide derivative is a paramagnetic species, as would be expected for a mononuclear octahedral Ni^{2+} complex. These results illustrate the exploitation of these compounds as magnetic sensors.

New chromogenic and fluorescent chemosensors based on bithienyl-imidazo-anthraquinone chromophores were studied in collaboration with Raposo and co-workers [81]. Compounds **59–61** represented in Scheme 19, were synthesized from 1,2-diaminoanthraquinone and the appropriate formyl-1-bithiophene, through an imine intermediate [81]. The sulfur donor atom in these compounds was introduced as in the flexible ligands **57** and **58** by the thiophene ring.

All compounds gave yellow solutions in acetonitrile. Upon interaction with negative charge anions such as, CN^- , H_2PO_4^- , CH_3COO^- , Cl^- , Br^- and I^- , any changes were observed in both absorption and fluorescence emission.

A remarkable red shift in the absorption from yellow to pink, and an increase of the fluorescence emission intensity was observed upon addition of fluoride for compounds **59–61**, see Fig. 38A. This effect is due to the deprotonation of the NH in the imidazole ring which can be achieved by the F^- .

The pink basic form of these compounds was explored as a chemosensor for metal ions. The original yellow color of the acidic form of the compounds is restored and the fluorescence quenched upon addition of Zn^{2+} , Cu^{2+} and Hg^{2+} , see Fig. 38. Association constants of the metal complexes were obtained by metal titrations. The titration plateau was achieved for 1:2 metal to ligand, in the case of Cu^{2+} and Hg^{2+} and 1:1 for Zn^{2+} .

In Fig. 38B the interaction with Hg^{2+} ions is shown. The stronger interaction was obtained for compound **59** with Hg^{2+} suggesting the involvement of the metal ion by the oxygen from the quinone ring and N from the imidazole unit, and the involvement of the sulfur from the thiophene ring.

In summary, the pink color of the solution observed upon fluoride addition changes to yellow or gold upon metal complexation giving an “OFF-ON-OFF”, yellow-pink-yellow, reversible colorimetric reaction (See Fig. 38).

9. Conclusions and outlook

The polyamine-based chemosensors reported in this review cover essentially the work carried out by the authors at the REQUIMTE in the New University of Lisbon in collaboration with the Universities of Florence (Italy), Valencia (Spain), Santiago de Compostela (Spain), Autonomous of Barcelona (Spain) and Minho (Portugal). Polyamine-based chemosensors were privileged, because they are very convenient to operate in water, the ubiquitous solvents in particular have application in biological systems. On the other hand, polyamine-based chemosensors have a severe drawback, because they are poor receptors for hard metals and by consequence some attempts to render these units more versatile were carried out through the incorporation of O, S and P atoms. However some of these mixed chemosensors are poorly soluble in water and by consequence the design of mixed receptors soluble in water is a necessary task to take into account in the future work.

It is expectable that the scientific community will continue to pay attention to this area of research due to the extended applications of chemosensors as: new imaging agents, development of new indicators to operate in water, in biomedical imaging and drug development, molecular devices and machines in nanoscale devices for recognition events, and intercalation into the DNA, proteins, etc.

Acknowledgements

We would like to thank our co-workers and all collaborators for their contribution to this research program, the FCT-MCTES/FEDER (Portugal) through projects POCTI/32442/2000, POCTI/QUI/47357/2002, POCTI/QUI/55519/2004, POCTI/QUI/57735/2004 and PDTC/QUI/66250/2006, the Xunta de Galiza (Spain) project PGIDT04PXIB2091PR as well as the European Commission project HPTN-CT-2000-00029 for financial support. Figures 5 and 29 have been reproduced by permission of the Royal Society of Chemistry on behalf of the Centre National de la Recherche Scientifique, and Figures 13, 14, 15, 16, 18, 25 and 38 were reprinted with permission from American Chemical Society.

References

- [1] L.R. Sousa, J.M. Larson, *J. Am. Chem. Soc.* 99 (1977) 307.
- [2] A.P. De Silva, *J. Chem. Soc. Chem. Commun.* (1986) 1709.
- [3] M.E. Huston, K.W. Haider, A.W. Czarnik, *J. Am. Chem. Soc.* 110 (1988) 4460.
- [4] A.W. Czarnik, *Acc. Chem. Res.* 27 (1994) 302.
- [5] (a) J. Costamagna, G. Ferraudi, B. Matsuhira, M. Campos-Vallete, J. Canales, M. Villagrán, J. Vargas, M.J. Aguirre, *Coord. Chem. Rev.* 196 (2000) 125; (b) J.D. Chartres, L.F. Lindoy, G.V. Meehan, *Coord. Chem. Rev.* 216/217 (2001) 249; (c) W. Radecka-Paryzek, V. Patroniak, J. Lisowski, *Coord. Chem. Rev.* 249 (2005) 2156; (d) L. Lomozik, A. Gasowska, R. Bregier-Jarbowska, R. Jastrzad, *Coord. Chem. Rev.* 249 (2005) 2335.
- [6] (a) P.A. Vigato, S. Tamburini, *Coord. Chem. Rev.* 248 (2004) 1717; (b) P.A. Vigato, S. Tamburini, L. Bertolo, *Coord. Chem. Rev.* 251 (2007) 1311; (c) S. Brooker, *Coord. Chem. Rev.* 222 (2001) 33.
- [7] (a) K.M.C. Wong, V.W.W. Yam, *Coord. Chem. Rev.* 251 (2007) 2477; (b) S.E. Angell, C.W. Rogers, Y. Wang, M.O. Wolf, W.E. Jones, *Coord. Chem. Rev.* 250 (2006) 1829; (c) P.J. Jiang, Z.J. Guo, *Coord. Chem. Rev.* 248 (2004) 205; (d) C.W. Rogers, M.O. Wolf, *Coord. Chem. Rev.* 233 (2002) 341; (e) S.S. Sun, A.J. Lees, *Coord. Chem. Rev.* 230 (2002) 171; (f) C. Bargossi, M.C. Fiorini, M. Montalti, L. Prodi, N. Zacheroni, *Coord. Chem. Rev.* 208 (2000) 17; (g) B. Valeur, I. Leray, *Coord. Chem. Rev.* 205 (2000) 3; (h) A. Prasanna de Silva, D.B. Fox, A.J.M. Huxley, T.S. Moody, *Coord. Chem. Rev.* 205 (2000) 41; (i) L. Prodi, F. Bolletta, M. Montalti, N. Zacheroni, *Coord. Chem. Rev.* 205 (2000) 59; (j) L. Fabbrizzi, M. Lichelli, G. Rabaioli, A. Taglietti, *Coord. Chem. Rev.* 205 (2000) 85; (k) M.H. Keefe, K.D. Benkstein, J.T. Hupp, *Coord. Chem. Rev.* 205 (2000) 201; (l) E.J. O’Neil, B.D. Smith, *Coord. Chem. Rev.* 20 (2006) 3068.
- [8] (a) E.J. O’Neil, B.D. Smith, *Coord. Chem. Rev.* 250 (2006) 3068; (b) R. Martínez-Mañez, F. Sancenón, *Chem. Rev.* 103 (2003) 4419; (c) T. Gunnlaugsson, M. Glynn, G.M. Tocci, P.E. Kruger, F.M. Pfeffer, *Coord. Chem. Rev.* 250 (2006) 3094; (d) V. Amendola, L. Fabbrizzi, F. Foti, M. Lichelli, C. Mangano, P. Pallavicini, A. Poggi, D. Sacchi, A. Taglietti, *Coord. Chem. Rev.* 250 (2006) 273.
- [9] E.U. Askaya, M.E. Huston, A.W. Czarnik, *J. Am. Chem. Soc.* 112 (1990) 7054.
- [10] L. Prodi, M. Montalti, N. Zacheroni, F. Dallavalle, G. Folesani, M. Lanfranchi, R. Corradini, S. Paglari, R. Marchelli, *Helv. Chim. Acta* 84 (2001) 690.
- [11] G. Farruggia, S. Lotti, L. Prodi, M. Montalti, N. Zazzheroni, P.B. Savage, V. Trapani, P. Sale, F.I. Wolf, *J. Am. Chem. Soc.* 128 (2006) 334.
- [12] C. Lodeiro, F. Pina, A.J. Parola, A. Bencini, A. Bianchi, C. Bazzicalupi, S. Ciattini, C. Giorgi, A. Masotti, B. Valtancoli, J.S. Melo, *Inorg. Chem.* 40 (2001) 6813.
- [13] R. Aucejo, J. Alarcón, E. García-España, J.M. Llinares, K.L. Marchin, C. Soriano, C. Lodeiro, M.A. Bernardo, F. Pina, J. Pina, J.S. de Melo, *Eur. J. Inorg. Chem.* (2005) 4301.
- [14] A.P. de Silva, H.Q.N. Gunarate, T.T. Gunnlaugson, A.J.M. Huxley, C.P. McCoy, J.T. Rademacher, T.E. Rice, *Chem. Rev.* 97 (1977) 1515.
- [15] A.P. de Silva, H.Q.N. Gunarate, P.L.M. Lynch, *J. Chem. Soc., Perkin Trans. 2* (1995) 685.
- [16] (a) S.A. de Silva, A. Zavaleta, D.E. Baron, O. Allam, E.V. Isidor, N. Kashimura, J.M. Percapio, *Tetrahedron Lett.* 38 (1997) 2237; (b) S.A. de Silva, B. Amorelli, D.C. Isidor, K.C. Loo, K.E. Crooker, Y.E. Pena, *Chem. Commun.* (2002) 1360.
- [17] L. Fabbrizzi, F. Gatti, P. Pallavicini, L. Parodi, *New J. Chem.* (1998) 1403.
- [18] (a) S. Sole, F.P. Gabba, *Chem. Commun.* (2004) 1284; (b) Y. Al Shihadeh, A. Benito, J.M. Lloris, R. Martínez-Mañez, T. Pardo, J. Soto, D.M.D. Martínez, *Polyhedron* 19 (2000) 1867; (c) C.G. Bangcuyo, U. Evans, M.L. Myrich, U.H.F. Bunz, *Macromolecules* 34 (2001) 7592; (d) T. Gunnlaugsson, A.P. Davis, M. Glynn, *Chem. Commun.* (2001) 2556; (e) M.C. Aragoni, M. Arca, F. Demartin, F.A. Devillanova, F. Isaia, A. Garau, V.

- Lipollis, F. Jalali, U. Shamsipur, L. Tei, A. Yari, G. Verani, *Inorg. Chem.* 41 (2002) 6623;
(f) E.M. Nolan, S.J. Lippard, *Inorg. Chem.* 43 (2004) 8310.
- [19] M.A. Bernardo, A.J. Parola, F. Pina, E. García-España, V. Marcelino, S.V. Luis, J.F. Miravet, *J. Chem. Soc., Dalton Trans.* (1995) 993.
- [20] M.A. Bernardo, J.A. Guerrero, E. García-España, S.V. Luis, J.M. Llinares, F. Pina, J.A. Ramirez, C. Soriano, *J. Chem. Soc., Perkin Trans. 2* (1996) 2335.
- [21] S. Alves, F. Pina, M.T. Albelda, E. García-España, C. Soriano, S. Luis, *Eur. J. Inorg. Chem.* (2001) 405.
- [22] E.A. Chandross, C.J. Dempster, *J. Am. Chem. Soc.* 92 (1970) 3586.
- [23] J.A. Sclafani, M.T. Maranto, T.M. Sisk, S.A. Van Arman, *Tetrahedron Lett.* 37 (1996) 2193.
- [24] M.T. Albelda, M.A. Bernardo, P. Díaz, E. García-España, J.S. de Melo, F. Pina, C. Soriano, S.V. Luis, *Chem. Commun.* (2001) 1520.
- [25] J.S. Melo, M.T. Albelda, P. Díaz, E. García-España, C. Lodeiro, S. Alves, J.C. Lima, F. Pina, C. Soriano, *J. Chem. Soc., Perkin Trans. 2* (2002) 991.
- [26] J.S. Melo, J. Pina, F. Pina, C. Lodeiro, A.J. Parola, J.C. Lima, M.T. albelda, M.P. Clares, E. García-España, *J. Phys. Chem. A* 107 (2003) 11307.
- [27] M.P. Clares, J. Aguilar, R. Aucejo, C. Lodeiro, M.T. Albelda, F. Pina, J.C. Lima, A.J. Parola, J. Pina, J.S. Melo, C. Soriano, E. García-España, *Inorg. Chem.* 43 (2004) 6144.
- [28] A. Bencini, A. Bianchi, C. Lodeiro, A. Masotti, A.J. Parola, F. Pina, J.S. Melo, B. Valtancoli, *Chem. Commun.* (2000) 1639.
- [29] A. Bencini, E. Berni, A. Bianchi, P. Fornasari, C. Giorgi, J.C. Lima, C. Lodeiro, M.J. Melo, J.S. Melo, A.J. Parola, F. Pina, J. Pina, B. Valtancoli, *Dalton Trans.* (2004) 2180.
- [30] R. Aucejo, J. Alarcón, E. García-España, J.M. Llenares, K.L. Marchin, C. Soriano, C. Lodeiro, M.A. Bernardo, F. Pina, J. Pina, J.S. De Melo, *Eur. J. Inorg. Chem.* (2005) 4301.
- [31] A.J. Parola, J.C. Lima, F. Pina, J. Pina, J.S. de Melo, C. Soriano, E. García-España, R. Aucejo, J. Alarcón, *Inorg. Chim. Acta* 360 (2007) 1200.
- [32] (a) T. Koike, T. Abe, M. Takahashi, K. Ohtani, E. Kimura, M. Shiro, *J. Chem. Soc., Dalton Trans.* 8 (2002) 1764;
(b) S. Aoki, K. Sakurama, N. Matsuo, Y. Yamada, R. Takasawa, S.I. Tanuma, M. Shiro, K. Takeda, E. Kimura, *Chem. Eur. J.* 12 (2006) 9066.
- [33] M.T. Albelda, P. Díaz, E. García-España, J.C. Lima, C. Lodeiro, J.S. de Melo, A.J. Parola, F. Pina, C. Soriano, *Chem. Phys. Lett.* 353 (2002) 63, See also erratum *Chem. Phys. Lett.* 362 (2002) 179.
- [34] (a) P.N.W. Baxter, *J. Org. Chem.* 66 (2001) 4170;
(b) Y. Chen, Q.L. Fan, P. Wang, B. Zhang, Y.Q. Huang, G.W. Zhang, X.M. Lu, H.S.O. Chan, W. Huang, *Polymer* 47 (2006) 5228;
(c) A.M. Costero, S. Gil, M. Parra, N. Huguet, Z. Allouni, R. Lakhmir, A. Atlamsani, *Eur. J. Org. Chem.* (2008) 1079;
(d) J.C. Loren, J.S. Siegel, *Ang. Chem. Int. Ed.* 40 (2001) 754;
(e) C. Goze, G. Ulrich, L. Charbonniere, M. Cesario, T. Prange, R. Ziessel, *Chem. Eur. J.* 9 (2003) 3748;
(f) W. Leslie, A.S. Batsanov, J.A.K. Howard, J.A.G. Williams, *Dalton Trans.* (2004) 623;
(g) M. Schmitt, V. Kalsani, R.S.K. Kishore, H. Colfen, J.W. Bats, *J. Am. Chem. Soc.* 127 (2005) 11544;
(h) B. Song, G.L. Wang, M.Q. Tan, J.L. Yuan, *J. Am. Chem. Soc.* 128 (2006) 13442;
(i) S.M. Brombosz, A.J. Zuccherro, R.L. Phillips, D. Vazquez, A. Wilson, U.H.F. Bunz, *Org. Lett.* 22 (2007) 4519;
(j) M.V. Del Pozo, C. Alonso, F. Pariente, E. Lorenzo, *Anal. Chem.* 77 (2005) 2550.
- [35] C. Bazzicalupi, A. Bencini, A. Bianchi, C. Giorgi, V. Fusi, B. Valtancoli, M.A. Bernardo, F. Pina, *Inorg. Chem.* 38 (1999) 3806.
- [36] A. Bencini, M.A. Bernardo, A. Bianchi, V. Fusi, C. Giorgi, F. Pina, B. Valtancoli, *Eur. J. Inorg. Chem.* 11 (1999) 1911.
- [37] C. Bazzicalupi, A. Bencini, A. Bianchi, L. Borsari, A. Danesi, C. Giorgi, C. Lodeiro, P. Mariani, F. Pina, S. Santarelli, A. Tamayo, B. Valtancoli, *Dalton Trans.* (2006) 4000.
- [38] J. Pina, J.S. de Melo, F. Pina, C. Lodeiro, J.C. Lima, A.J. Parola, C. Soriano, M.P. Clares, M.T. Albelda, R. Aucejo, E. García-España, *Inorg. Chem.* 44 (2005) 7449.
- [39] C. Lodeiro, A.J. Parola, F. Pina, C. Bazzicalupi, A. Bencini, A. Bianchi, C. Giorgi, A. Masotti, B. Valtancoli, *Inorg. Chem.* 40 (2001) 2968.
- [40] C. Andá, C. Bazzicalupi, A. Bencini, A. Bianchi, P. Fornasari, C. Giorgi, B. Valtancoli, C. Lodeiro, A.J. Parola, F. Pina, *Dalton Trans.* (2003) 1299.
- [41] C. Bazzicalupi, A. Bencini, E. Berni, A. Bianchi, A. Danesi, C. Giorgi, B. Valtancoli, C. Lodeiro, J.C. Lima, F. Pina, M.A. Bernardo, *Inorg. Chem.* 43 (2004) 5134.
- [42] *Probe Design and Chemical Sensing: Topics in Fluorescence Spectroscopy 4*, J.R. Lakowicz ed. New York (1994).
- [43] Z. Murtaza, Q. Chang, G. Rao, H. Lin, J.R. Lakowicz, *Anal. Biochem.* 247 (1997) 216.
- [44] (a) S.C. Rawle, P. Moore, N.W. Alcock, *J. Chem. Soc., Chem. Commun.* (1992) 684;
(b) N.W. Alcock, A.J. Clarke, W. Errington, A.M. Josceanu, P. Moore, S.C. Rawle, P. Sheldon, S.M. Smith, M. Turonek, *J. Chem. Soc., Chem. Commun.* (1996) 281.
- [45] C. Lodeiro, F. Pina, A.J. Parola, A. Bencini, A. Bianchi, C. Bazzicalupi, S. Ciatini, C. Giorgi, A. Masotti, B. Valtancoli, J.S. de Melo, *Inorg. Chem.* 40 (2001) 6813.
- [46] (a) F. Pina, M. Ciano, L. Moggi, V. Balzani, *Inorg. Chem.* 24 (1985) 844;
(b) F. Pina, M. Maestri, R. Ballardini, Q.G. Mulazzani, M. D'angelantonio, V. Balzani, *Inorg. Chem.* 25 (1986) 42;
(c) A. Bianchi, K. Bowman-James, E. García-España, *Supramolecular Chemistry of Anions*, Wiley-VCH, New York, 1997.
- [47] (a) F. Peter, M. Gross, M.W. Hosseini, J.-M. Lehn, R.B. Sessions, *J. Chem. Soc., Chem. Commun.* (1981) 1067;
(b) F. Peter, M. Gross, M.W. Hosseini, J.-M. Lehn, *Electroanal. Chem.* 144 (1983) 279.
- [48] E. García-España, M. Micheloni, P. Paoletti, A. Bianchi, *Inorg. Chim. Acta* 102 (1985) L9.
- [49] A. Bencini, A. Bianchi, E. García-España, M. Giusti, S. Mangani, M. Micheloni, P. Orioli, P. Paoletti, *Inorg. Chem.* 26 (1987) 3902.
- [50] J. Aragó, A. Bencini, A. Bianchi, A. Domenech, E. García-España, *J. Chem. Soc., Dalton Trans.* (1992) 319.
- [51] A. Bianchi, A. Domenech, E. García-España, S. Luis, *Anal. Chem.* 65 (1993) 3137.
- [52] A. Juris, M.T. Gandolfi, M.F. Manfrin, V. Balzani, *J. Am. Chem. Soc.* 98 (1976) 1047.
- [53] D.M. Roundhill, *Photochemistry and Photophysics of Metal Complexes*, Plenum Press, New York, 1994.
- [54] M.P. Clares, C. Lodeiro, D. Fernández, A.J. Parola, F. Pina, E. García-España, C. Soriano, R. Tejero, *Chem. Commun.* (2006) 3824.
- [55] M.T. Albelda, J. Aguilar, S. Alves, R. Aucejo, P. Díaz, C. Lodeiro, J.C. Lima, E. García-España, F. Pina, C. Soriano, *Helv. Chim. Acta* 86 (2003) 3118.
- [56] (a) J. Azéma, C. Galaup, C. Picard, P. Tisnès, O. Ramos, O. Juanes, J.C. Rodríguez-Ubis, E. Brunet, *Tetrahedron* 56 (2000) 2673;
(b) C. Galaup, M.-C. Carrié, P. Tisnès, C. Picard, *Eur. J. Org. Chem.* (2001) 2165.
- [57] (a) J.-C. Rodríguez-Ubis, B. Alpha, D. Plancherel, J.-M. Lehn, *Helv. Chim. Acta* 67 (1984) 2264;
(b) B. Alpha, J.-M. Lehn, G. Mathis, *Angew. Chem. Int. Ed. Engl.* 26 (1987) 266;
(c) C. Roth, J.-M. Lehn, J. Guilhem, C. Pascard, *Helv. Chim. Acta* 78 (1995) 1895, and references therein.
- [58] (a) F. Barigelletti, L. De Cola, V. Balzani, P. Belser, A. von Zelewsky, F. Vögtle, F. Ebmeyer, S. Grammenudi, *J. Am. Chem. Soc.* 111 (1989) 4662;
(b) V. Balzani, R. Ballardini, F. Bolletta, M.T. Gandolfi, A. Juris, M. Maestri, M.F. Manfrin, L. Moggi, N. Sabbatini, *Coord. Chem. Rev.* 125 (1993) 75, and references therein;
(c) N. Sabbatini, M. Guardigli, J.-M. Lehn, *Coord. Chem. Rev.* 123 (1993) 201;
(d) V. Balzani, A. Credi, M. Venturi, *Coord. Chem. Rev.* 171 (1998) 3, and references therein.
- [59] (a) C. Bazzicalupi, A. Bencini, A. Bianchi, C. Giorgi, V. Fusi, A. Masotti, B. Valtancoli, A. Roque, F. Pina, *Chem. Commun.* (2000) 561;
(b) C. Bazzicalupi, A. Bencini, E. Berni, A. Bianchi, C. Giorgi, V. Fusi, B. Valtancoli, A. Lodeiro, A. Roque, F. Pina, *Inorg. Chem.* 40 (2001) 6172.
- [60] T.E. Mallouk, J.S. Krueger, J.E. Mayer, C.M.G. Dymond, *Inorg. Chem.* 28 (1989) 3507.
- [61] (a) W. De Horrocks, D.R. Sudnick, *J. Am. Chem. Soc.* 101 (1979) 334;
(b) W. De Horrocks, D.R. Sudnick, *Acc. Chem. Res.* 14 (1981) 384.
- [62] R.M. Izatt, K. Pawlak, J.S. Bradshaw, R.L. Bruenig, *Chem. Rev.* 91 (1991) 1721.
- [63] (a) C. Bazzicalupi, A. Bencini, A. Bianchi, E. Faggi, C. Giorgi, C. Lodeiro, E. Oliveira, F. Pina, B. Valtancoli, *Inorg. Chim. Acta* 361 (2008) 3410;
(b) K.M.K. Swamy, S.K. Kwon, H.N. Lee, S.M.S. Kumar, J.S. Kim, J. Yoon, *Tetrahedron Lett.* 48 (2007) 8683;
(c) M. Hershinkel, W.F. Silverman, I. Sekler, *Mol. Med.* 7–8 (2007) 331;
(d) A. Ojida, Y. Miyahara, A. Wongkongkatep, S. Tamaru, K. Sada, I. Hamachi, *Chem. Asian J.* 1 (2006) 555.
- [64] (a) H. Dugas, *Bioorganic Chemistry: A Chemical Approach to Enzyme Action*, Springer, New York, 1996;
(b) W. Kühnbrandt, *Nature* 5 (2004) 282;
(c) R. Sharma, C. Rensing, B.P. Rosen, B. Mitra, *J. Biol. Chem.* 275 (2000) 3873;
(d) Z. Hou, B. Mitra, *J. Biol. Chem.* 278 (2003) 28455.
- [65] C. Bazzicalupi, A. Bencini, A. Bianchi, A. Danesi, C. Giorgi, C. Lodeiro, F. Pina, S. Santarelli, B. Valtancoli, *Chem. Commun.* (2005) 2630.
- [66] R.G. Pearson, *J. Am. Chem. Soc.* 85 (1963) 3533.
- [67] (a) M. Vicente, C. Lodeiro, H. Adams, R. Bastida, A. De Blás, D.E. Fenton, A. Macías, A. Rodríguez, T. Rodríguez-blás, *Eur. J. Inorg. Chem.* (2000) 1015;
(b) E. Bértolo, R. Bastida, D.E. Fenton, C. Lodeiro, A. Macías, A. Rodríguez, *J. Alloys Compd.* 323/324 (2001) 155;
(c) C. Lodeiro, R. Bastida, E. Bértolo, A. Macías, A. Rodríguez, *Polyhedron* 22 (2003) 1701;
(d) E. Bértolo, R. Bastida, D.E. Fenton, C. Lodeiro, A. Macías, A. Rodríguez, *J. Inclusion Phen. Macro. Chem.* 45 (2003) 155;
(e) C. Lodeiro, R. Bastida, E. Bértolo, A. Macías, A. Rodríguez, *Trans. Metal. Chem.* 28 (2003) 388;
(f) C. Lodeiro, R. Bastida, E. Bértolo, A. Macías, A. Rodríguez, *Inorg. Chim. Acta* 343 (2003) 133;
(g) C. Lodeiro, J.L. Capelo, E. Bértolo, R. Bastida, *Z. Anorg. Allg. Chem.* 630 (2004) 1110;
(h) C. Lodeiro, R. Bastida, E. Bértolo, A. Rodríguez, *Can. J. Chem.* 82 (2004) 443;
(i) C. Lodeiro, E. Bértolo, J.L. Capelo, R. Bastida, *Z. Anorg. Allg. Chem.* 630 (2004) 914;
(j) M. Vicente, R. Bastida, C. Lodeiro, A. Macías, A.J. Parola, L. Valencia, S.E. Spey, *Inorg. Chem.* 42 (2003) 6768.
- [68] A.W. Czarnik, *Fluorescent Chemosensors for Ion and Molecule Recognition*, American Chemical Society, Washington, DC, 1993.
- [69] E. Oliveira, M. Vicente, L. Valencia, A. Macías, E. Bértolo, R. Bastida, C. Lodeiro, *Inorg. Chim. Acta* 360 (2007) 2734.
- [70] A. Freiria, R. Bastida, L. Valencia, A. Macías, C. Lodeiro, H. Adams, *Inorg. Chim. Acta* 359 (2006) 2383.

- [71] (a) C. Lodeiro, J.L. Capelo, J. Inclusion Phen. Macro. Chem. 49 (2004) 249;
(b) C. Lodeiro, J.C. Lima, J. Parola, J.S. Seixas de Melo, J.L. Capelo, A. Tamayo, B. Covelo, B. Pedras, Sens. Actuators B: Chem. 115 (2006) 276;
(c) M. Vazquez, M.R. Bermejo, J. Sanmartín, A.M. García-Deibe, C. Lodeiro, J. Mahía, J. Chem. Soc., Dalton Trans. 6 (2002) 870;
(d) M.R. Bermejo, M. Vazquez, J. Sanmartín, A.M. García-Deibe, M. Fondo, C. Lodeiro, New J. Chem. 26 (2002) 1365, and references therein;
(e) M. Fondo, A.M. García-Deibe, N. Ocampo, J. Sanmartín, M.R. Bermejo, E. Oliveira, C. Lodeiro, New J. Chem. 32 (2008) 247.
- [72] (a) A. Gocmen, C. Erk, J. Inclusion Phen. Mol. Rec. Chem. 26 (1996) 67;
(b) C. Erk, A. Gocmen, Talanta 53 (2000) 137.
- [73] (a) W.S. Kim, J.M. You, B.J. Lee, Y.K. Jang, D.E. Kim, Y.S. Kwon, J. Nanosci. Nanotechnol. 6 (2006) 3637;
(b) W.L. Jia, D.R. Bai, T. McCormick, Q.D. Lius, M. Motala, R.Y. Wang, C. Seward, Y. Tao, S.M. Wang, Chem. Eur. J. 10 (2004) 994;
(c) P.F. Wang, Z.R. Hong, Z.Y. Xie, S.W. Tong, O.Y. Wong, C.S. Lee, N.B. Wong, L.S. Hung, S.T. Lee, Chem. Commun. (2003) 1664;
(d) E.M. Gross, J.D. Anderson, A.F. Slaterbeck, S. Thayumanavan, S. Barlow, Y. Zhan, S.R. Marder, H.K. Hall, M.F. Nabor, J.F. Wang, E.A. Mash, N.R. Armstrong, R.M. Wightman, J. Am. Chem. Soc. 122 (2000) 4972.
- [74] (a) A. Tamayo, C. Lodeiro, L. Eschiche, J. Casabó, B. Covelo, P. González, Inorg. Chem. 44 (2005) 8105;
(b) A. Tamayo, J. Casabó, L. Eschiche, P. González, C. Lodeiro, A.C. Rizzi, C.D. Brondino, M.C.G. Passeggi, R. Kivekäs, R. Sillampää, Inorg. Chem. 46 (2007) 5665.
- [75] A. Tamayo, E. Oliveira, B. Covelo, J. Casabó, L. Eschiche, C. Lodeiro, Z. Anorg. Allg. Chem. 633 (2007) 1809.
- [76] A. Tamayo, B. Pedras, C. Lodeiro, L. Eschiche, J. Casabó, J.L. Capelo, B. Covelo, R. Kivekäs, R. Sillampää, Inorg. Chem. 46 (2007) 7818.
- [77] A. Tamayo, L. Eschiche, J. Casabó, B. Covelo, C. Lodeiro, Eur. J. Inorg. Chem. (2006) 2997.
- [78] B. Pedras, H.M. Santos, L. Fernandes, B. Covelo, A. Tamayo, E. Bértolo, J.L. Capelo, T. Avilés, C. Lodeiro, Inorg. Chem. Commun. 10 (2007) 925.
- [79] A. Tamayo, J. Casabó, L. Eschiche, C. Lodeiro, B. Covelo, C.D. Brondino, R. Kivekäs, R. Sillampää, Inorg. Chem. 45 (2006) 1140.
- [80] A. Tamayo, L. Eschiche, C. Lodeiro, J. Ribas-Ariño, J. Ribas, B. Covelo, J. Casabó, Inorg. Chem. 45 (2006) 7621.
- [81] R.M.F. Batista, E. Oliveira, S.P.G. Costa, C. Lodeiro, M.M.M. Raposo, Org. Lett. 9 (2007) 3201.